CZECH TECHNICAL UNIVERSITY IN PRAGUE

FACULTY OF MECHANICAL ENGINEERING

BACHELOR'S THESIS

2022
GABRIEL
BRUNO PARREIRA

CZECH TECHNICAL UNIVERSITY IN PRAGUE

FACULTY OF MECHANICAL ENGINEERING

DEPARTMENT OF MATERIAL ENGINEERING

BACHELOR THESIS

DESIGN AND CHARACTERIZATION OF MAGNETIC SHAPE MEMORY-BASED

MICROPUMP

AUTHOR: Gabriel Bruno Parreira

STUDY PROGRAM: Theoretical Fundamentals of Mechanical Engineering

SUPERVISOR: Ing. Stanislav Krum, Ph.D.

PRAGUE 2022

BACHELOR'S THESIS ASSIGNMENT

I. Personal and study details

Student's name: **Bruno Parreira Gabriel**   Personal ID number: **491078**

Faculty / Institute: **Faculty of Mechanical Engineering**

Department / Institute: **Department of Materials Engineering**

Study program: **Theoretical Fundamentals of Mechanical Engineering**

Branch of study: **No Special Fields of Study**

II. Bachelor's thesis details

Bachelor's thesis title in English:

Design and characterization of magnetic shape memory-based micropump

Bachelor's thesis title in Czech:

Návrh a charakterizace mikropumpy na bázi magnetické tvarové paměti

Guidelines:

1) Literature research
2) Magnetic shape memory material preparation
3) Design and construction of the micropump
4) Evaluation of construction and material suitability

Bibliography / sources:

[1] A. Armstrong, Material Design, Processing, and Engineering Requirements for Magnetic Shape Memory Devices, Boise State University Theses and Dissertations (2020)
[2] D. T. Chiu, A. J. deMello, D. Di Carlo, P. S. Doyle, C. Hansen, R. M. Maceiczyk, et al., Small but Perfectly Formed, Successes, Challenges, and Opportunities for Microfluidics in the Chemical and Biological Sciences, Chem 2 (2017), no. 2, 201–223

Name and workplace of bachelor's thesis supervisor:

Ing. Stanislav Krum, Ph.D.   Department of Materials Engineering FME

Name and workplace of second bachelor's thesis supervisor or consultant:

Date of bachelor's thesis assignment: **30.03.2022**   Deadline for bachelor thesis submission: **31.07.2022**

Assignment valid until: _____

Ing. Stanislav Krum, Ph.D.	prof. RNDr. Petr Špatenka, CSc.	prof. Ing. Michael Valášek, DrSc.
Supervisor's signature	Head of department's signature	Dean's signature

III. Assignment receipt

Date of assignment receipt	Student's signature

Statement

I declare that I have worked out this thesis independently assuming that the results of the thesis can also be used at the discretion of the supervisor of the thesis as its co-author. I also agree with the potential publication of the results of the thesis or of its substantial part, provided I will be listed as the co-author.

Prague, ……………………………

………………………………………………
Signature

Abstract:

The present work was dedicated to the study of the effects of shot-peening (SP) on the twinning stress (TS) and amount of "spring-back" (SB) on 10M modulated NiMnGa magnetic shape memory alloy (MSMA). It then uses such treated samples as an active element in a micro-fluidic pump. Section 1 is a brief introduction that clearly presents what this work is aiming to achieve as well as a brief summary of what will be dealt with in each subsequent section. Section 2 deals with a brief history of shape memory in general and magnetic shape memory effect specifically as well as a short explanation on the how this effect is produced; it also briefly talks about microfluidics challenges and how the MSMA has been previously used for other pump designs. Section 3 goes on to explain how the MSMA material is prepared for use in the pump. The resulting TS and SB obtained by the SP process with different parameters is also presented in this section. Section 4 deals with the design and construction of the microfluidic pump utilizing the MSMA as an active element. It also briefly goes into the technological process for producing Polydimethylsiloxane (PDMS) parts, which were used as sealant material in the pump. Finally, section 5 is dedicated to evaluating if the work achieved the results which it proposed to achieve in section 2.

Keywords: Magnetic Shape Memory Alloy, Microfluidic pump, Twining Stress, Shot-Peening.

List of Abbreviations and Symbols Used:

MSMA   Magnetic Shape Memory Alloy

PDMS   Polydimethylsiloxane

TB   Twin Boundary

TS   [MPa]   Twinning stress

SP   Shot Peening

EP   Electropolishing

SB   [1]   Spring-Back

MFIS   [1]   Magnetic Field Induced Strain

FDM   Fused Deposition Modelling

PETG   Polyethylene terephthalate glycol

Acknowledgments

Contents

1. Introduction:

This work in based on making improvements on a Magnetic Shape Memory alloy (henceforth MSMA) based microfluidic pump, which will be used for demonstration purposes by the Physics department of the Czech Academy of Science. In addition to making improvements to the general construction and working of the pump, the design was also modified in such a way that the samples utilized in the pump could be easily replaced, and thus allowing for the pump to be used for other applications (for example for cycle testing of samples). The accomplishment of such task involves an exploration related to the preparation of the MSMA sample as well as an assessment of the suitability of any given sample for the pump application.

The present work was also concerned with exploring the effects of surface treatments on the twinning stress of the 10M NiMnGa MSMA. More specifically the process of shot-peening (SP) was employed to cause surface damage on samples of the MSMA. This treatment is applied to stabilize the desired twin boundary structure on the surface of the material so it will have the desired behavior when utilized in the microfluidic pump. In addition to the micro-peening, the samples were also electropolished and the effects of that procedure were also briefly commented upon.

One side-project that had to be taken on to improve the pump performance was a brief exploration on polydimethylsiloxane (henceforth PDMS) production, specially concerning the proper casting of the PDMS. Although there will not be a dedicated section for discussing this topic, I will briefly comment on the procedures utilized for producing PDMS parts as well as a commentary on future studies that will be done involving the PDMS mechanical properties.

In section 2, the theoretical background related to the MSMA and the general technologies related to microfluidic devices as well as previous works related to MSMA-based micro pumps is presented. The general principles behind magnetic shape memory effect are explained, the effects of surface treatment, and the challenges related to the production of microfluidic devices are all included in this section.

Section 3 is dedicated to the MSMA treatments and its effects on the shape of the stress-strain curve as well as on the twinning stress of the sample, and on the amount of "spring-back" that the sample has. Mostly in this section it is shown how changes in the parameters of the micro-peening procedure affect the final behavior of the sample, and how the electropolishing can be used to return the sample back to its pre-treatment state.

In section 4 the design of the micropump is presented. Some aspects concerning the choice of materials and general geometry are explained in relation to the final goal that the pump is supposed to achieve. A brief presentation on different iterations and future designs will also be presented. In here I also talk briefly about the PDMS and the production of parts made from it.

Finally, section 5 is a general evaluation of the work. Here, the question: "Was the initial goal accomplished successfully?" Will be answered based on the results obtained in section 2 and 3 and in accordance to the proposed objectives presented in the introduction.

2. Shape Memory Effect:

Shape memory alloys were first discovered in 1932 by Arne Ölander. Later, new metallic, and polymeric materials were discovered to have the shape memory effect. Initially the most common materials to present the shape memory effect did so under changes in temperature of the material, which in turn caused the material to undergo a phase change (from Austenite to

martensite and back). In 1996 Ullakko et.al made the first report of a magnetic shape memory alloy with high strains; this was a NiMnGa alloy. Now this is the most common MSMA studied and it is also the alloy used for this project. [1]

2.1. The MSM Effect:

Upon cooling the NiMnGa alloy goes through phase transformation and settles on an FCC crystal structure, which is typically called its Austenite state; This austenite state has a relatively high degree of symmetry. When the material is further cooled when in its austenite state, it undergoes a phase transformation into martensite. The martensitic phase has a tetragonal crystal structure and is therefore less symmetric than the austenite phase. Critically, this new martensite structure has different lengths of c-axis and a-axis; the ratio between them ($\varepsilon_0 = c/a$) is a critical parameter for the magnetic shape memory effect [1].
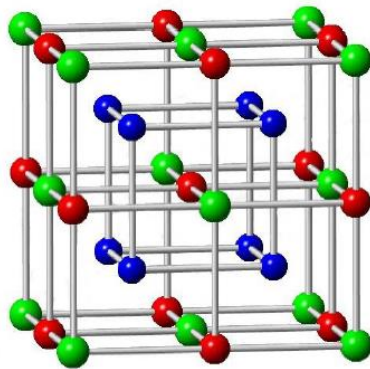
Figure 1. Austenite structure of stochiometric NiMnGa alloy. The gallium, manganese and Nickel atoms are represented in green, red and blue, respectively [1].

Because $\varepsilon_0 \neq 1$ in the martensite structure, the crystal structures can be in many different orientations, which results in what is called twin domains; the twin microstructures form in order to accommodate the internal strains caused by the shear transformation to martensite [1]. Each of

these domains is separated from a different neighboring domain by a twin boundary. These boundaries can move through the material when a stress is applied to it, and how easily these boundaries move is what is called the **twinning stress** (TS) of a particular sample of the material; this twinning stress is another important parameter in the ability of a sample presenting MSM effect [1], [2].
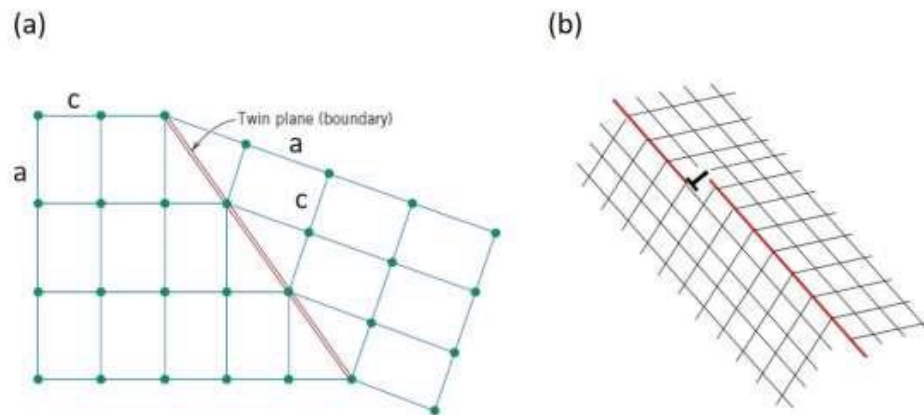
Figure 2. (a) Two different variants of martensitic structure separated by twin boundaries, with the "a" and "c" axis of each indicated. (b) Illustration of how the twin boundary can move by the switching of the "a" and "c" axes. It is possible to see that one variant is the "reflection" of the other across the twin boundary [2].

So far, we discussed the physical characteristics of the material's crystal structure that allows the twin variants to change from one type to the other, namely the twinning stress, however such discussion is valid in general for any type of applied stress and is not exclusively related to stresses applied by a magnetic field. The parameter that deals with the applicable stress by a magnetic field in the materials is the magneto stress. The magneto stress is nothing more than a stress applied to a MSMA sample by a magnetic field; typically, the maximal applicable magneto stress to a 10M NiMnGa alloy is 3 MPa. It is then clear that the value of the magneto stress has to be higher than the value of the twinning stress, otherwise is not possible to create enough stress in

the material to induce the movement of the twin boundaries; the value of ε_0, the twinning stress, and the magneto stress are all related to the power output available to a given MSM sample [1].

Non-modulated NiMnGa alloys has a twinning stress bigger than the magneto stress applicable to a given sample, and thus it cannot be used for magnetic shape memory effects. The most commonly studied and used alloy is the modulated 10M NiMnGa alloy (10M). That is because the 10M alloy has a relatively high applicable magneto stress (3.0 MPa), the lowest reported twinning stresses (1 MPa, with reports as low as 0.5 MPa), and it has an austenite transformation starting temperature (As) above room temperature, with the highest reported temperature being 353 K, and for those reasons it is also the type of alloy used in this work [1], [2].

Previously, we have discussed how ε_0 can influence the movement of twin boundaries across the material and what are the necessary conditions to be able to do that through the application of a magnetic field (i.e., the magneto stress has to be higher than the twinning stress); however, we have yet to explain what is the physical mechanism behind the creation of this stress only by the magnetic field, and how we can actually promote twin boundary movements only by the application of a magnetic field. The characteristic responsible for this is the magnetic anisotropy of the material [2].

Although most crystalline materials present some degree of magnetic anisotropy, this phenomenon becomes more relevant in single crystal materials, such as the MSMA utilized in this work. Magnetic anisotropy simply means that the material will more easily magnetize in the direction of one of the crystal axes (c-axis for this material) than the other. So, when a magnetic field is applied to the material, the c and a-axes change directions in such a way that the easily magnetized axis aligns with the applied magnetic field to the material. In order for the material to present any MSM effect, it is paramount that the Magnetic Anisotropy Energy (K_u), is greater than

the energy necessary for twin boundary motion (E_{tw}), any work done by the actuation (W) and any other energy that might oppose the movement of twin boundaries (E_0), as expressed in the following equation presented by Ullakko in 1996 [1]:

$$K_u > E_{tw} + W + E_0$$
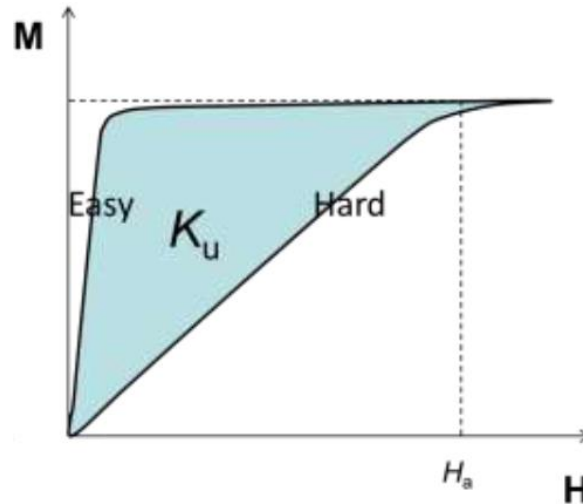
Figure 3. This graph shows measured magnetization curve along the easy axis (c-axis) and hard magnetization axis (a-axis). The x-axis shows the strength of applied magnetic field, and the y-axis, shows the magnetization of the material [2].

The magnetic anisotropy energy refers to the energy is the energy resulting from the difference in magnetization between the easy and hard axis of magnetization. The work done can roughly be linked to what we are looking for from the sample. There is, we want to use the energy available in the sample to perform some work, such as applying some force to a mechanism, or transporting fluid from one point to another, as what is done in the microfluidic pump.

In **Figure 3**, the magnetic anisotropy energy of the material (KU) can be determined as the area between the two magnetization curves. The change of axis direction causes a macroscopic strain in the material, called magnetic field induced strain (MFIS), and also changes the ratio between the different martensite variants in the material; in fact, if we leave the sample in a strong

enough magnetic field, the sample will only have the variant that favorably aligns with the applied

magnetic field and any other variant will be completely "consumed [2]."
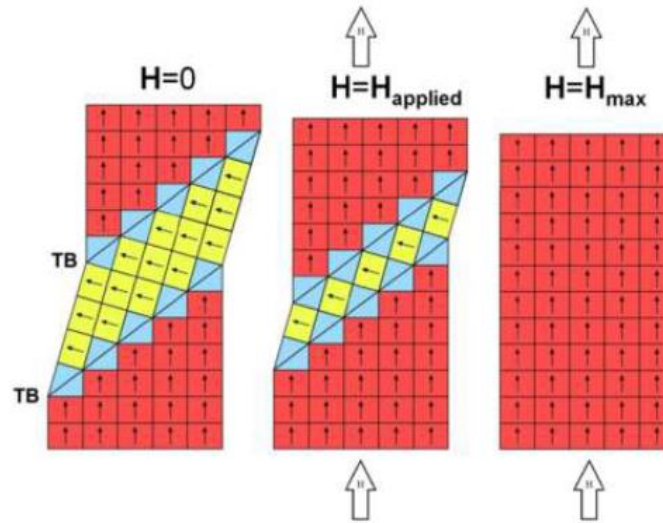
Figure 4. Transformation of one twin variant into another by the application of a magnetic field. As the magnetic field increases, more and more of the twin variants' easy axis of magnetization align with the direction of the applied field, and eventually the favorable variant "consumes" the unfavorable one [2].

To conclude this discussion on the basic mechanisms behind the MSM effect, I must

discuss the important process of sample "training." If we place a sample in a magnetic field, the

variant that is "favorably" aligned to the magnetic field will "consume" the other variant and

become the only one present in the sample as illustrated in **Figure 4**. Similar processes that change

the proportion of variants present, or maybe change the distribution of variants across the material,

are part of what is called the material's "training." The training of a particular sample can greatly

influence not only how it behaves under the magnetic field, but also how resistant the materials

will be to repeated actuation. The material can be trained not only by the application of a magnetic

field but also by performing some surface treatment. Such treatments were the ones more often

used and investigated in this work, and their effects and applications will be discussed in the next

section [2].

(a)   (b)
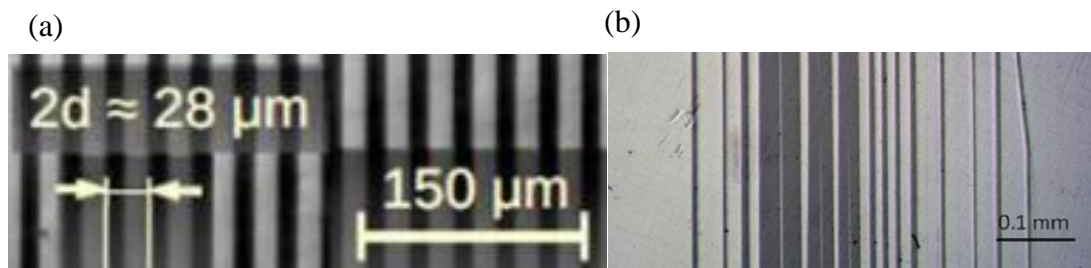
Figure 5. (a) An example of a sample with fine twin structure; (b) an example of a sample with localized variation of twin structures [2], [3].

In **Figure 5**, one can see that (a) has a more uniform distribution of both variants in a "fine twin" structure, while in (b) the sample is dominated by the gray looking variant with the presence of some of the "black" variant in the middle.

### 2.1.1. Effects of Surface Modification:

For the purposes of this work, surface modifications in NiMnGa alloys serve 2 main purposes: first is to stabilize the desired arrangement of twins and twin boundaries microstructures on the surface of the sample; second is to increase the resistance of the sample to actuation fatigue [4]. Although the surface modification has its advantages, unfortunately, it also has some undesirable consequences.

The surface modifications prevent fatigue damage on the surface of the samples by creating obstacles for the propagation of fractures. However, the surface defects that accomplish that, are also serving as obstacles to the desirable propagation of the twin boundaries that are responsible for the MFIS in our material. Thus, any surface modification, be it for increasing resilience or any other desired modifications, must be carefully balanced so that the twinning stress of the treated sample does not become higher than the applicable magneto stress [2], [5], [4].

There are various ways in which the surface can be modified. We can introduce surface damage by the shot-peening method (the main method investigated in this work), mechanical

polishing and grinding. These methods are used to introduce surface damage on the sample and to stabilize the surface microstructure, while the electropolishing can be used to "reset" the sample to its original state, with almost no damage on its surface [2], [5].
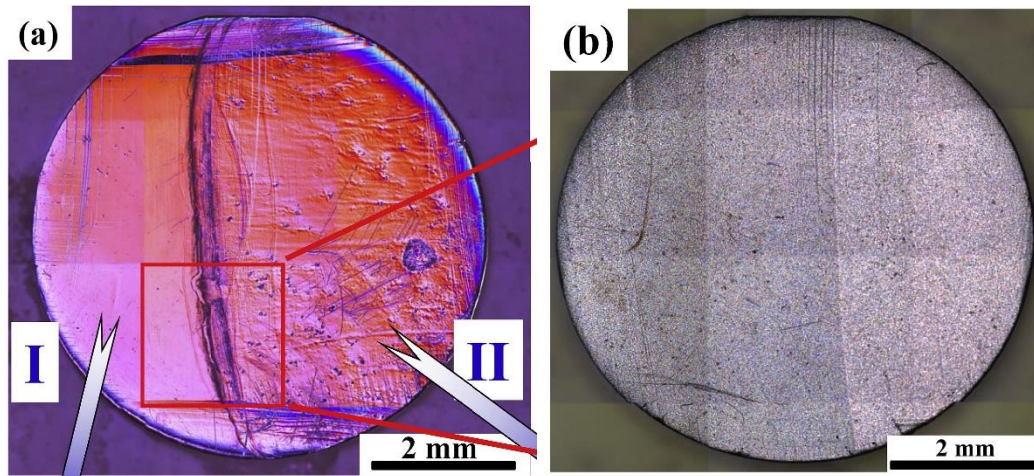
Figure 6. Example of samples with different treatments. (a) sample that had half of it (left) mechanically polished and the other half (right) electropolished. (b) sample that was micro-peened. The shadows in (b) are caused by sample inclination during microscopy [4].

All these surface modifications are part of the training of the MSM sample. The material without this or other forms of training will most likely not perform according to the desired outcomes. For the purpose of the pump, we apply surface modifications to obtain a fine twin structure on the surface of the sample. This structure helps to increase the fatigue life of the sample, which is crucial for a device that is repeatedly actuated by the magneto stress, as is the case in the pump. This configuration allows for relatively high MFIS, while keeping the fatigue resistance high, unlike a single variant MSM sample, which presents higher strains, but have considerably lower fatigue resistance. The fine-twin structure also creates the type of strains necessary for utilization of the material in the micro-fluidic pump application [2].

Another effect that we are trying to achieve with the shot-peening, is the setting of a surface stress that is acting to restore the samples original shape. That is important because any change on

the materials shape does not spontaneously revert back to the original state of the sample (pseudo-plastic deformation). In order for the sample to return to its original configuration after some stress is applied to it, we must apply a "restoring" stress on the sample. Thus, not only we have to properly constraint the sample from all sides, we also must help to return the sample to its original configuration by inducing a residual surface stress that is trying to keep the sample in its original shape once a deformation is applied to it; such behavior is what I will refer to as the "Spring-Back" (SB) of the sample, and how much of the SB occurred was one of the parameters measured in this work [2]. The amount of spring-back is measured because it has to be present to some degree for proper functioning of the pump for the motives I just touched upon previously; however, it has to be noted that I was not able to find in the literature any minimum or "recommended" amount of spring back that a sample must have in order for the pump to work properly.

2.2. Techniques in Microfluidics:

Microfluidics is defined as a set of technologies utilized for manipulating small quantities of fluids within channels with dimensions in the micrometer scale [6]. Microfluidics' advantages are mostly exploited in the biomedical and biochemistry fields, but it also has been useful to the cosmetic industry, and the printing industry. Most of microfluidic techniques have been developed in the biochemistry and biomedical industries due to its advantages in performing research in those areas. The advantages of microfluidics are many, among them are fast processing time and the utilization of less reagents and space, which increases financial savings as well as making it possible to run multiple experiments at once in a small environment. But there are more advantages than just that; microfluidic techniques also increases precision and control of experiments as well as of the experimental environment through general fluid properties at such small scales [7], [8].

Despite its many advantages, microfluidics still faces some challenges, especially concerning the manufacturing of the devices used in those applications. Many of the traditional manufacturing techniques are often too slow and require highly controlled environments to manufacture microfluidic devices with the necessary precision. More recently, 3D printing techniques have been used to manufacture microfluidic devices, and new techniques have been developed or adapted for such purposes [8].

Although promising, 3D printing is just starting to be exploited in microfluidics applications, and currently the most popular technique for fabrication is still the soft lithography for manufacturing devices made of PDMS. Although suitable for making very small features, PDMS is far from being an ideal material for all applications, and the techniques used for manufacturing devices with it, limit the technology to planar devices rather than fully exploit 3-dimensional structures. Even with the now available 3D printing technology, many of the microfluidic devices are still limited to 2-dimensions, as the 3D-printed parts are many times used only as casts for the PDMS and other materials. However, the improvement of old and creation of new 3D-printing technologies have made it possible to make truly 3-dimensional microfluidic devices [8], [9].
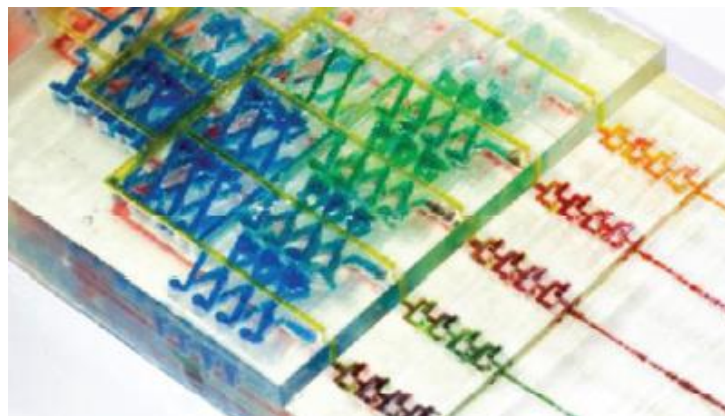
Figure 7. Example of 3D-printed microfluidic device used for mixing of different solutions [8].

Although not the only method, stereolithography (SLA) printing is especially suitable for microfluidic devices, as it can make the smallest features with a relatively high precision, especially when compared to fused deposition modelling (FDM) printing. However, SLA prints require some post processing, while FDM prints can be ready to go as soon as they are done printing; despite that, the amount of post processing and raw material necessary for SLA prints are still far smaller than the resources needed for traditional manufacturing, and it also waste less material than a traditional manufacturing method [8], [9].

2.3. MSMA-Based Micropumps:

As described in the previous section, microfluidics is the set of technologies to manipulate small quantities of fluid within channels in the micrometer scale [6]. Since small quantities of fluid are being delt with, it is also necessary to have some means of pumping such small quantities in a reliable and repeatable manner. In modern practice the pumping of fluid is accomplished either by utilizing peristaltic pumps, by some pump based on piezoelectric principles, or by some sort of syringe pump [10], [11]. While those technologies are already well stablished and have the advantage of utilizing technologies already existent from other applications, none of them have all of the desirable characteristics of a microfluidic pump, since they are either mechanically complex, or require external connections which makes its integration with other microfluidic devices problematic. The MSM-based micro pump solves many of these problems by being a mechanically simple device with a single active part (namely the MSMA sample itself), which does not require direct electronical connection, since the sample is actuated (i.e. a strain is induced in the sample) by the application of a magnetic field, while being reliable on the amount of fluid delivered and being able to work with relatively high back pressures [12].

What is being proposed to be accomplished in this work is an assessment of the parameters affecting the results of the shot-peening treatment and the utilization of the appropriately treated samples to construct a microfluidic pump. The various advantages of magnetic shape memory alloys have been used for microfluidic pumps for a long time. Besides the advantages already mentioned in the previous paragraph, the MSMA-based microfluidic pump also can easily be integrated in lab on a chip application. The MSM pump also can very precisely and repeatedly deliver discrete quantities of fluid due to its working mechanism, which will be explained in this section [12].

The principle behind the fluid transfer in the MSM pump is related to a local contraction caused by a magnetic field which is localized in a specific section of the sample. Such contraction follows the applied magnetic field to a sample, thus, by rotating a magnet under the sample, we can make the contraction move along the sample from one point to another. As the magnet rotates, the field moves along the sample, which contracts the volume of the sample's section within the field. Such contraction forms a cavity in which a fluid can be accommodated and, as that cavity moves along the length of the sample, we transfer a discrete quantity of fluid from one point to another. From that we can realize that the fluid transfer is not done in a continuous smooth fashion but in discrete packages [2], [3], [12]. The schematics in **Figure 8** bellow illustrate the mechanism I just described.
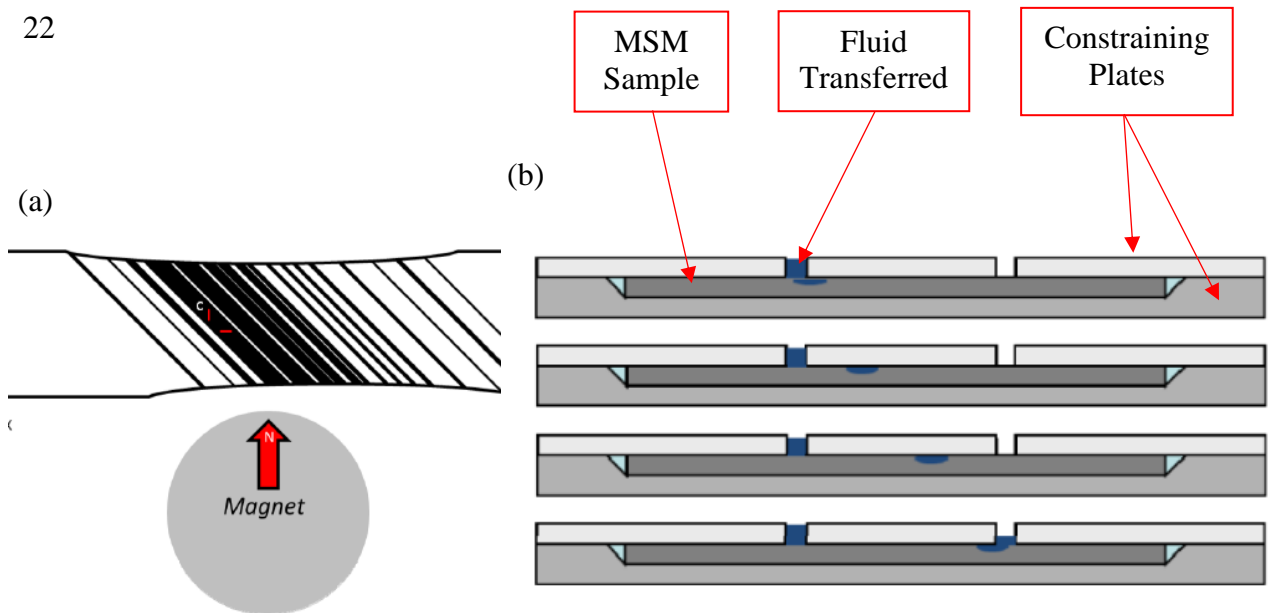
Figure 8. (a) a schematic representation of how a cavity is formed in the sample as a result of a stress created by the magnetic field from the cylindrical, radially magnetized magnet; (b) a schematics of how the fluid transfer takes place in the pump[3].

Another thing we must note from the mode of actuation of the pump, is that one rotation of the magnet corresponds with two "pumping cycles", that is, one full rotation produces 2 cavities that transport the fluid [12]. The first use of MSM in micropump application was reported by Ullakko in 2012 [3].
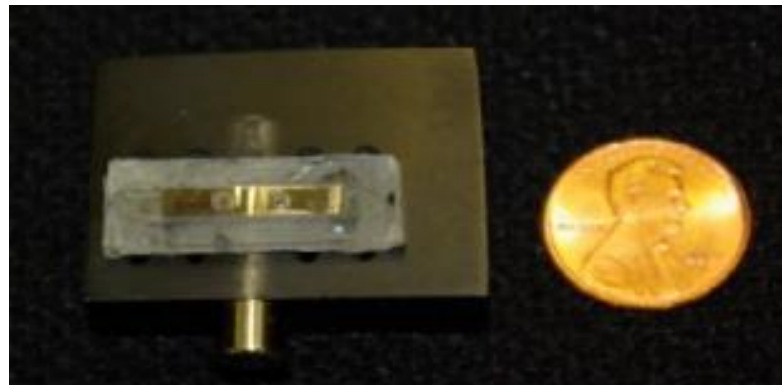
Figure 9. Ullakko et al. original micropump design. The pump is set by a U.S. penny for size comparison, one can also observe the cylindrical magnet below the sample [3].

The original design proposed by Ullakko had the advantage of being extremely simple, making it an ideal blueprint for further proposed designs [12]. However, that and subsequent designs suffered from inadequate sealing which cause large variations in flow rate, and decreased

the operational pressure. Some other designs were made by clamping the sample between plates, which did improve some aspects of the pump, but also made the pumping pressure and stability highly dependent on the clamping force, which introduces another difficulty in the design of a reliable pump. More recently, in 2018, a group of researches finally proposed a new design that properly sealed, and fully constrained the MSM sample, in such a way that highly stable flow under relative high pressures were obtained [12].
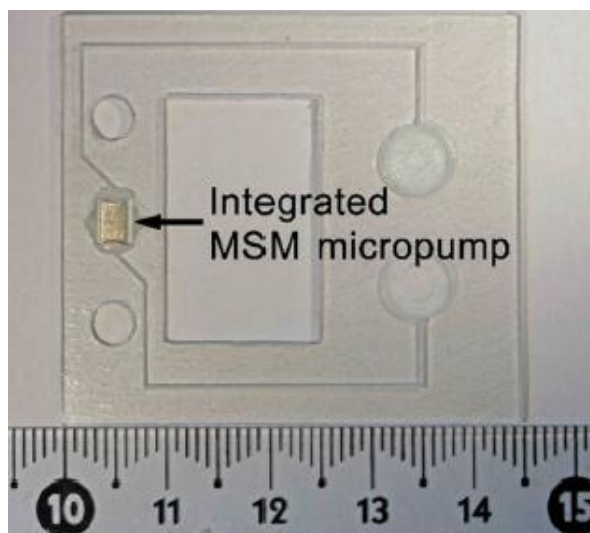
Figure 10. Micropump design integrated in a mock lab in a chip application. This is the most recent design the author of the present paper is aware of, made in 2018 [12].

The 2018 design by Saren's team, is the one with the best flow characteristics that the author of this work is aware of. Although there are some room for improvements on that pump, the primary goal of this work is not to attempt improving on such design, but rather to make a pump that is to be used for demonstration purposes and which can still be functional while maintaining the possibility of easily replacing the samples in the pump. The possibility of easy sample replacement can then further be used to investigate other aspects of the MSM sample that can affect pump performance, as well to investigate other applications. One example of such application would be to use the pump to actuate the sample for a determined number of cycles or

for a determined amount of time, and assess how well a coating layer remains on the sample surface. Such application was not investigated in the present work and this paper is concerned with proposing a functional design of the pump as well as investigating how shot peening parameters affect the sample's twinning stress, and thus its suitability for use as an MSM material. After the pump design is improved, it will be used for material testing purposes and for demonstration purposes at the Physics Institute of the Czech Academy of Science (FZU).

3. Preparation of MSM Samples

## 3.1. MSMA as Active Element:

When an MSM sample is produced it is not yet ready to be used in the pump application. The material will contain coarse martensite twins on its surface, but for reliable performance in the pump, fine twin martensite is required; The fine twin is created by bending the sample, but if some stress is applied to the sample, the twin configuration in the sample will be changed and the fine twins will be lost as they do not reappear after the stress is removed; therefore, after the fine twins are created, they have to be stabilized by means of surface stress. The surface stress is generated by the process of shot-peeing [12].

3.2. MSM Sample Modification:

The MSM element was used as the active part of a microfluidic pump. In order to work properly, the element needs a special configuration on its surface of martensite twin boundaries; this is the so called fine-twin martensite. This configuration generates a specific type of strains that can be exploited for fluid transport as discussed in section two of this work.

Before I start the discussion on the treatments and procedure for obtaining and identifying a desirable sample, I will introduce some nomenclature to make the discussion simpler in the following explanation.
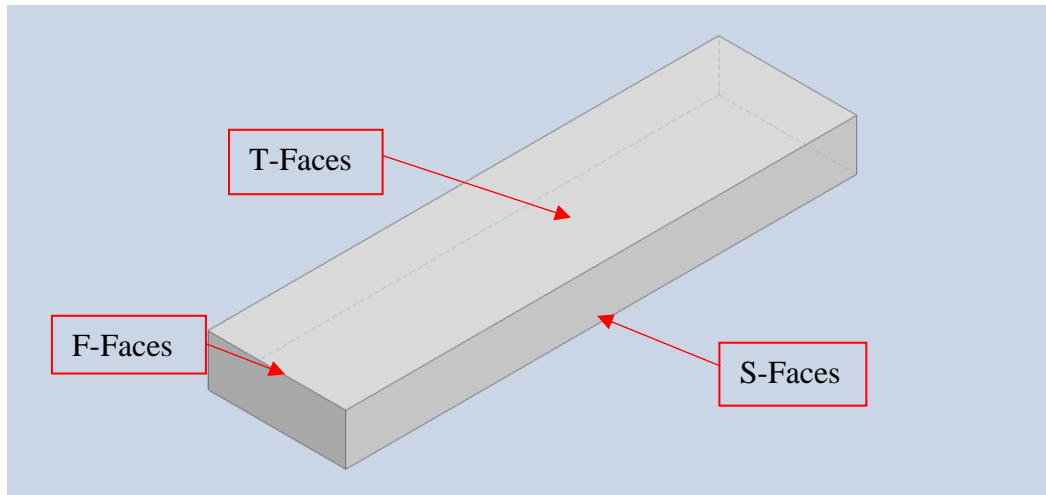
Figure 11. Schematic of the sample with labels for each of pair of faces in the sample.

Figure 11 shows how I will be referring to each pair of faces of the sample in the discussion that follows. Thus, the T-faces in the figure have dimensions of approximately 2.7 X 10 mm^2, the S-faces are 1 X 10 mm^2 and the F-Faces are 2.7 X 1 mm^2; henceforth, I will be referring to the faces according to the tags shown in **Figure 11**.

The fine twin structure can be obtained by bending a MSM sample that has coarse twin martensite, or that is homogeneous and has virtually no twin boundaries on its surface; however, if the sample is not treated, the fine twin martensite created by the bending is not stable. If an external load is applied to the MSM sample with the fine-twins, they will disappear and the sample will again have coarse twin martensite or become a single variant sample (depending on the stress applied to the sample). The shot-peening (SP) treatment is used to stabilize the fine-twin martensite that is necessary for the proper functioning of the pump. The twin configuration present on the

surface of the samples can be seen under a polarized light micrograph and the stress-strain (SS) curve of the sample also serves as an indicator of the twins' configuration and how stable they are.
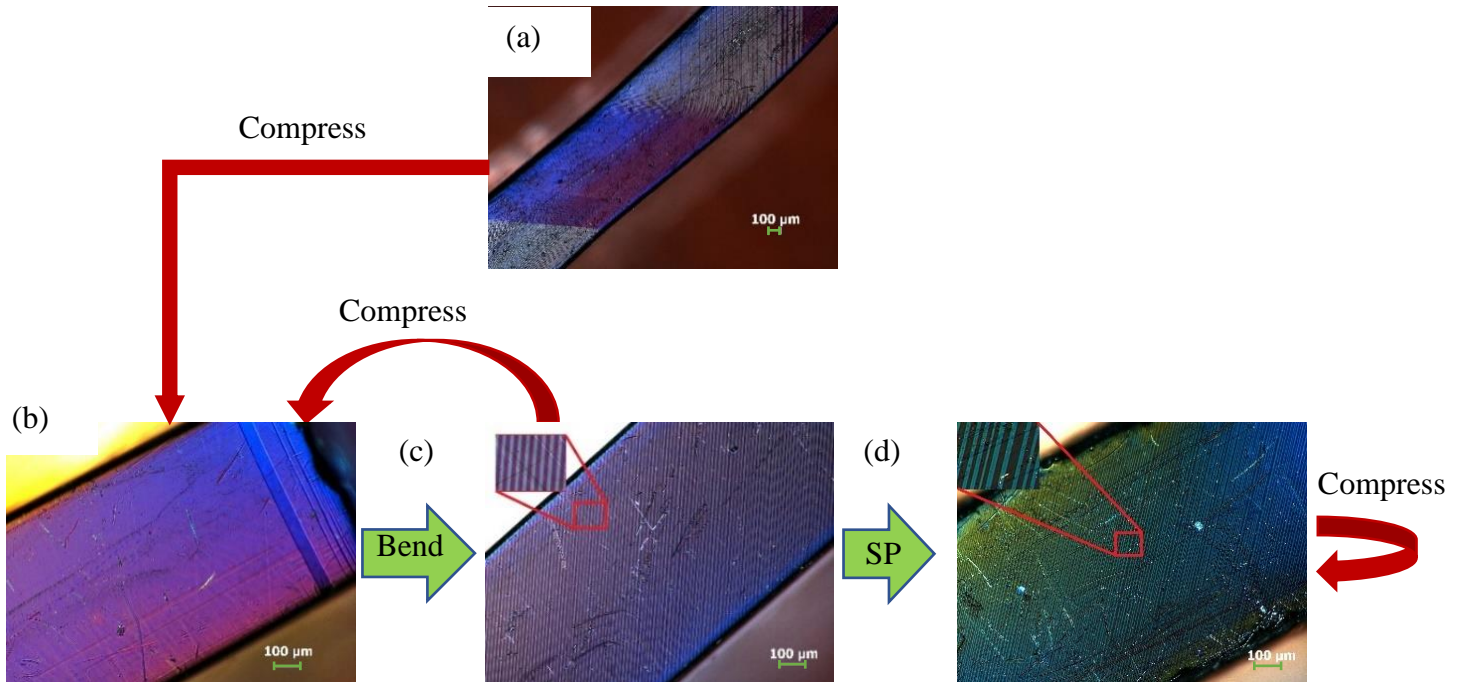
Figure 12. Schematics showing the effects of bending, stress application and shot-peening. The images are micrographs of the S-face in different samples using polarized light: (a) Sample with coarse twin structure; (b) sample with single variant martensite after having external stress applied to it; (c) sample with unstable fine-twin structure, and (d) sample with permanent fine-twin structure.

Figure 12 shows the different stages of the sample preparation. First, we have the sample with a coarse twin structure, then we bend it to obtain the fine-twins, and finally we apply the shot-peening treatment to make the fine-twin structure stable under load application and removal. The presence of the fine-twin structure is quite evident from micrograph imaging as shown in

Figure 12, however the distinguishing between a permanent fine-twin structure and an unstable one is more evident by evaluation of the stress-strain curve of the sample.
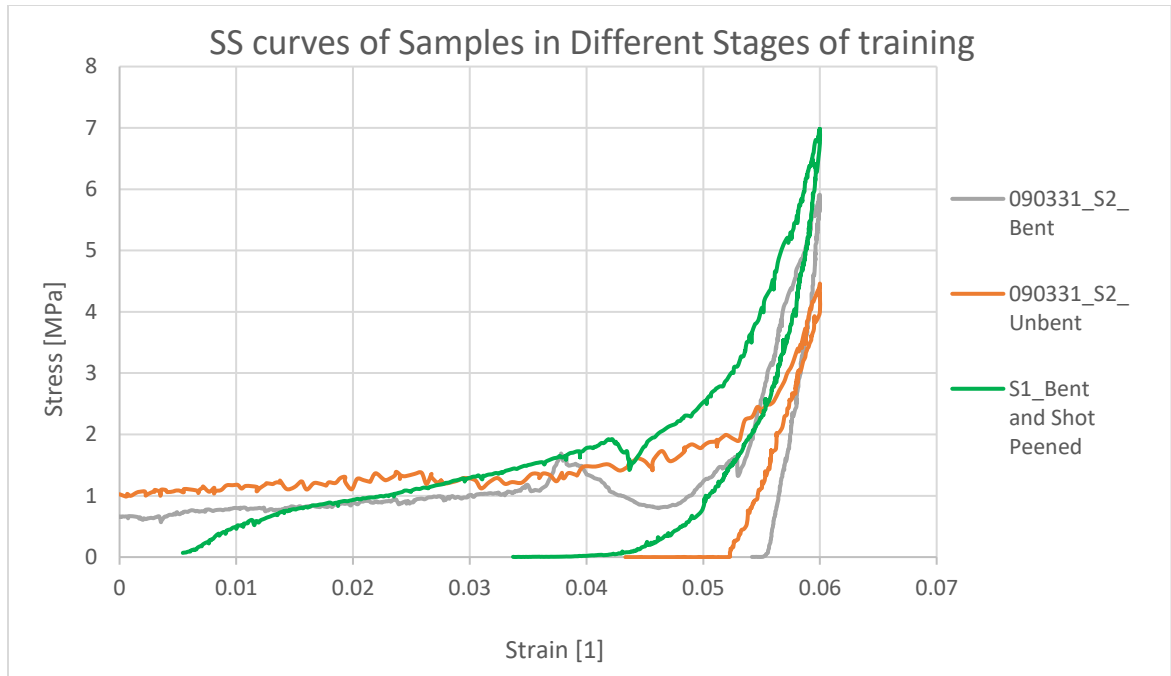
Figure 13. In this figure we have the SS results of samples in different states of treatment as shown in the chart's legend.

In **Figure 13** we have an example of the SS test results for different samples. What we are looking for is an elastic region after the stress stops being applied to the sample and a relatively low twinning stress. We can see that there is not much of a difference in behavior between the unbent sample and the bent sample before any treatment and that we have a relatively low twinning stress (how twinning stress was defined in this work is explained in section 3 and illustrated in **Figure 14**) once the strain is being removed from the sample, we can observe that the stress dependence on the strain follows a relatively steep straight line until the stress reaches 0 MPa. In the sample that was bent and subsequently shot-peened we can see that the twinning stress is higher than the samples in the previous states, but once the stress is being removed at the end of the SS test, the sample has some spring-back, with a visible reduction in the strain as the stress is being removed. The twinning stress, and the amount of spring-back of a sample, were the two criteria used to evaluate the suitability of a given sample to be used in the pump.

3.3. Experimental:

The samples were treated by shot-peening with different parameters. And the effects of the shot-peening on the twinning stress and on the spring-back of the samples was evaluated by a stress-strain (SS) test. The parameters being changed were the air pressure in the shot-peening device, and the discharge nozzle used in the shot-peening (see **Figure 17**).

The twining stress was measured because the value of the twinning stress has to be smaller than the maximal applicable magneto stress to the material; which, in the case of the material used in this experiment, is ~3 MPa. Thus, the twinning stress was evaluated to see if it would be below the 3 MPa value, and if it was, then the sample would be a good candidate for utilization in the pump. Besides the twinning stress, the amount of spring back was also measured.

The spring-back (SB) was measured because in order for the sample to work properly in the pump application, it is necessary that the fine-twin martensite configuration is present in the sample. As shown in **Figure 12**, the creation of that structure is relatively simple, but it also has to be stabilized; the SB of the sample serves as the indicator for such stability of the fine-twins. Although I did not find in literature a minimum amount of SB necessary for proper working on the pump, the measurement of its presence on the treated samples was still necessary to assess if the fine twins were stable. Furthermore, my hypothesis is that the amount of SB is somehow related to the pump performance and some of its pumping characteristics, so having the data on the amount of SB could be useful for future investigation on this hypothesis. However, this hypothesis was not investigated in the present work.

3.4. Methodology:

The samples studied were tested in the SS machine (**Figure 18**) before and after any shot-peening. For the testing, the sample was inserted in between the jaws of the SS machine and then the jaws were closed to gradually increase the displacement of the sample; as the displacement was being increased a **compressive stress** was being applied to the samples. When the force reached 14 N the jaws were slowly opened until the force applied to the sample reached 0 N. The stress-strain curve was then saved as a text file, which could then be used for further processing and evaluation. The machine was manually operated and the samples did not all have the same cross-section area, thus there were variations on the maximum stress applied to different samples.

After this initial characterization the samples were treated with the shot peening device. For the shot peening the sample was bent "inwards" towards the T-Face (**Figure 11**) that was going to be treated, then it was attached to the moving stage using double sided tape. The pressure and distance of the nozzle were set to the desired values with the help of a pressure gauge and a measuring tape respectively, then the sample was "centered" under the discharge nozzle. The parameters were set as follows in the different treatment modes:

Table 1. The table below shows the different parameters used for shot-peening treatments. Note that the speed with which the sample was being moved was not changed. Also, the distance between the sample and the nozzle was kept the same. The column referring to row numbers is added for easier reference of parameters further in the text.

Row	Pressure [Bar]	Nozzle	Distance [mm]	Moving Stage Speed [mm/s]
1	4	circular	~15	NA
2	1.5	circular	15	9
3	1	rectangular	15	9

One thing that can be noted in **Table 1**, is that the distance was not changed in the treatments being performed to the MSM samples. That is the case because before any treatments were performed to the samples, the parameters related to the distance of the nozzle to the moving stage where the sample was located was tested in an acrylic plate to check how the distance affected the width of the sand jet. Based on information available on the paper by Armstrong [2] and on the tests performed on the acrylic piece, the distance was set to 15 mm from the surface of the moving stage, as this allowed for coverage of the whole width of the sample with the sand stream. However, later on the rectangular nozzle was acquired (see **Figure 17**), which has a larger opening and likely it would be possible to have enough spread to cover the whole sample with a smaller distance between nozzle and moving stage, but I chose to keep the distance constant so that only the effects of orifice size would be affecting the final results of the shot-peening.

The speed of the moving stage was kept the same for all tests because even the maximum speed was somewhat slow; the maximum speed achievable by the moving stage was approximately 9 mm/s, and that was the speed used for all the treatments, except by a few that were done by hand as "test runs". The speed was kept to a maximum because the dwelling time under the sand stream could affect the amount of damage being done to the surface of the samples. Initially, the tests with the parameters shown in row 2 of **Table 1** were performed only on samples S3, S4 and S5. This is only because I was trying to save the samples that seemed to be in better conditions for further tests in a later time.

It also has to be noted that the first treatment using 4 bars of air pressure was performed only once to a single sample. This test was performed by hand before the automatic moving stage was available and it was performed only to have a "feel" of what pressure could be good for the

treatment process nonetheless the results from that will be presented in the results section. After the further literature investigation and tests, it was determined that the 1.5 bar pressure was a better setting for the shot-peening treatment. Finally, after a manual treatment with different parameters on sample S2, I was able to get some good results (as far as twinning-stress and spring-back were concerned) and thus I used the same settings to further treat sample 4. Those are the parameters shown on row 3 of **Table 1**. The pressure was reduced to 1 bar, and the nozzle was changed to the one depicted on **Figure 17.a**. With this I hoped to obtain less damage to the surface of the samples, so that I was able to better control the twinning stress while still having some level of spring-back in the sample.

On the table presented below, there is a list of the samples that were utilized for the experiments performed in this work. The samples were simply named as S (for sample) followed by a number (1, 2, 3, etc.). These numbers do not have any particular meaning related to the samples but I kept samples from a same batch as consecutive numbers. Furthermore, sample number 1 (S1), was significantly longer than the other samples and thus it was cut in half to produce 2 new samples which were numbered S1-1 and S1-2. Finally, all the samples have the composition: $Ni_{50}Mn_{28}Ga_{22}$, by atomic percentage. For heat treatment the samples were placed in quartz ampoules at 1273 K for 48 hours for homogenization and then there were subject to aging treatment at 1073 K for up to 24 hours. Finally, they were let to cool slowly in the furnace.

Table 2. Table showing the surface treatments applied to each of the samples. The table also includes the initial dimension of each sample before any electropolishing. Those dimensions were still used for the SS test as it was assumed that the electropolishing was not enough to make significant changes on the thickness.

Sample	Batch#	Treatments/Procedures performed on sample	Thickness [mm]	Width [mm]	Length [mm]
S1-1,2	NA	Cut in half by wire saw	0.95	2.40	20.9
S2	090331	Electropolished/Mechanically Polished/Electropolished	1.25	2.80	9.75
S3	090331	Electropolished	1.20	2.75	10.05
S4	090331	Electropolished	1.20	2.70	10.10
S5	090331	Electropolished	1.15	2.75	10.10
S6	NA	"Trimmed"/Shot peening/Electropolished	0.94	2.39	10.01

Once all the parameters were set and the sample was appropriately located with respect to the nozzle, the sample was moved out of the way of the sand stream, then the sand flow was started and the moving stage was set in motion in such a way that the whole length of the sample passed under the sand stream. The sample was then removed from the stage and acetone was used to remove any residual glue from it. After cleaning, the sample was tested again in the SS machine. If the sample presented the desirable elastic behavior shown in **Figure 13.c**, and had a twinning stress below 3 MPa, then the sample was a good candidate for utilization in the pump. Otherwise, if the desired behavior was not present, the sample was treated again according to the same procedure, provided that its twinning stress was not already above or equal to 3 MPa. In the case that the sample had too high of a twinning stress, then it was electropolished and treated again with different shot peening parameters. The limiting value is 3 MPa because for the particular material

being utilized in this work, the maximum magneto stress that is possible to apply to any given

sample is 3 MPa.

The following figure exemplifies how the evaluation of the data was done, and in the next

paragraphs there is a more detailed explanation of the procedure.
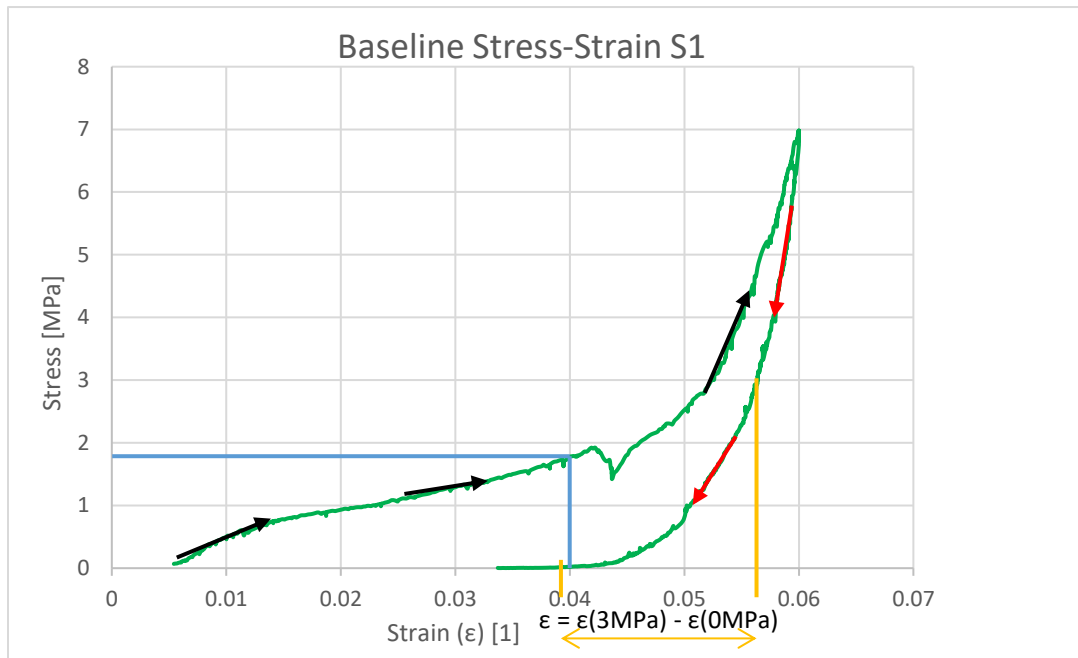
Figure 14. The graph is from a treated sample and exemplifies how the spring back and the twinning stress were measured. The blue lines are indicating the twinning stress reading; the yellow line and the equation by the yellow arrow are indicating how the spring-back was determined. The black arrows indicate the loading direction (sample being compressed) and the red arrows indicate the removal of the compressive stress.

To perform the evaluation of the results, the SS curves of each individual sample were

analyzed using Excel. To do that I shifted the strains in the samples such that the maximum strain

was at 0.06, this process is what I will be referring to as "normalizing" the SS curve. With a

normalized curve I then evaluated the twinning stress, which I defined as being the stress value at

0.04 strain, as demonstrated by the blue lines in **Figure 14**. The reading of twinning stress was

done by reading the stress directly out of the graph at strain 0.04. The point 0.04 of strain does not

have any particular meaning, the only reason it was chosen is because the strains on the untreated material generally should not exceed 0.06 and, when the treatment is applied, there is generally a maximum strain of about 0.03, so the strain of 0.04 is close to mean between 0.06 and 0.03 (more precisely mean would be 0.045, but 0.04 was easier to read directly from the graph and it is close enough to the mean value).

The spring-back strain was evaluated in the following manner: First, the value of the strain when the stress reached 3 MPa was read in the SS curve, then the strain value at 0 MPa stress upon the removal of the compressive stress was read; the spring-back is then defined as the difference between the strain at 3 MPa and 0 MPa when the load is being removed from the sample. Again, the values for these strains were read directly out of the graph produced from the data extracted from the stress-strain testing machine (see **Figure 18**). The reading is exemplified by the yellow lines and arrow, as well as by the equation in **Figure 14**. To determine a single value for the twinning stress and spring-back I took the average of two or three tests done in a given sample. The value of strain at 3 MPa was used because this value has the physical meaning that it is the maximum stress applicable to the sample utilizing only a magnetic field.

3.5. Equipment Used:

For the shot-peening treatment, a small sandblaster with glass beads of size from 50 to 70 μm was used. For initial tests, a nozzle with a circular opening with 0.8 mm diameter was used and for further tests a rectangular nozzle with opening 2.9 x 1.4 mm^2 was used. The sand blasting device was modified with an inhouse built moving stage for the MSM sample, which allowed for consistent linear movement in the blaster.
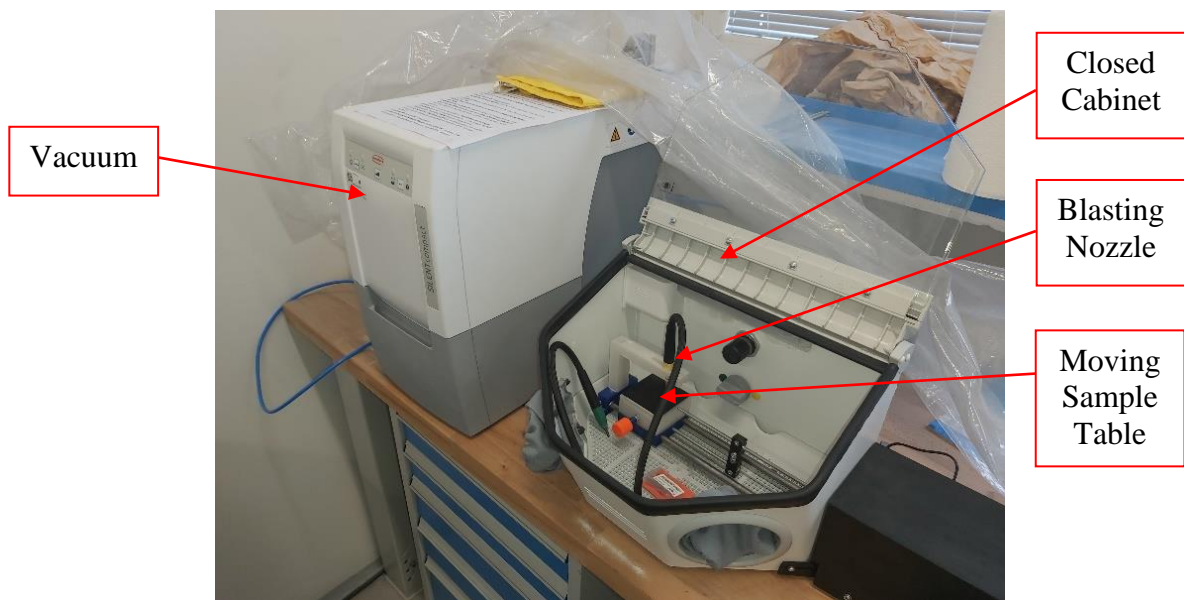
Figure 15. Sand Blasting device used to treat the MSM samples. With the carriage for movement inside.
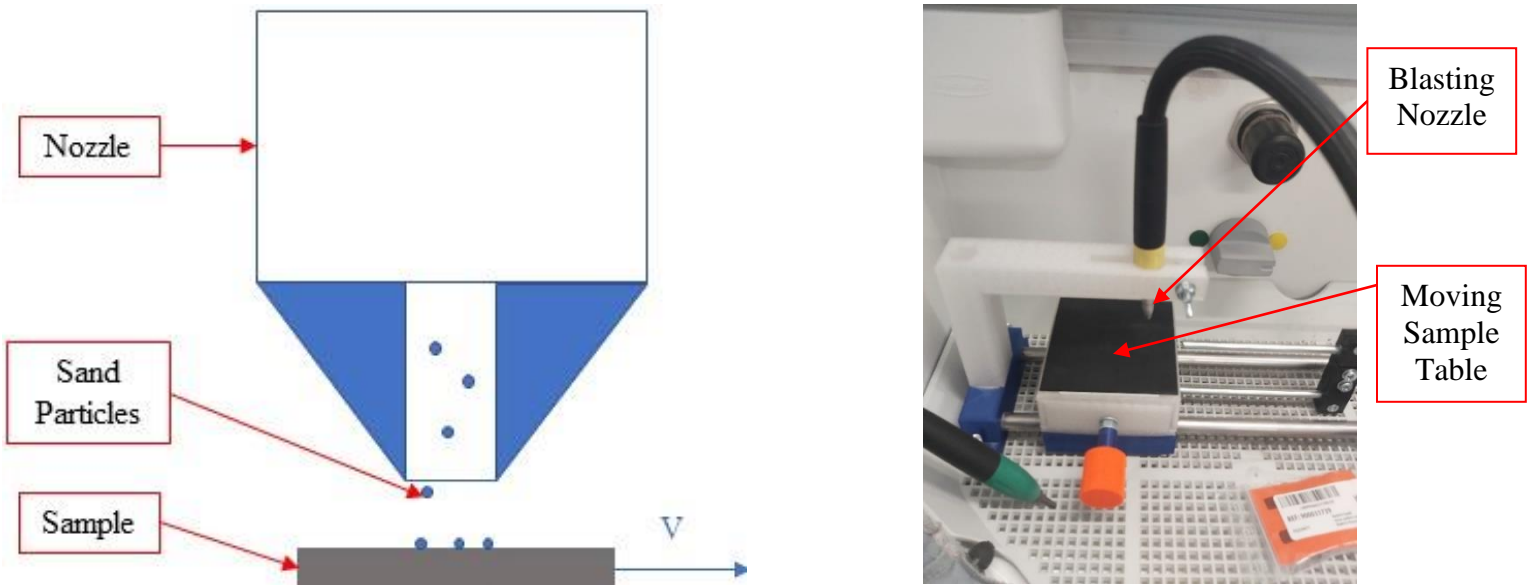
Figure 16. Carriage device for the MSM sample. (a) Schematic of shot-peening process; (b) picture of the actual device used.
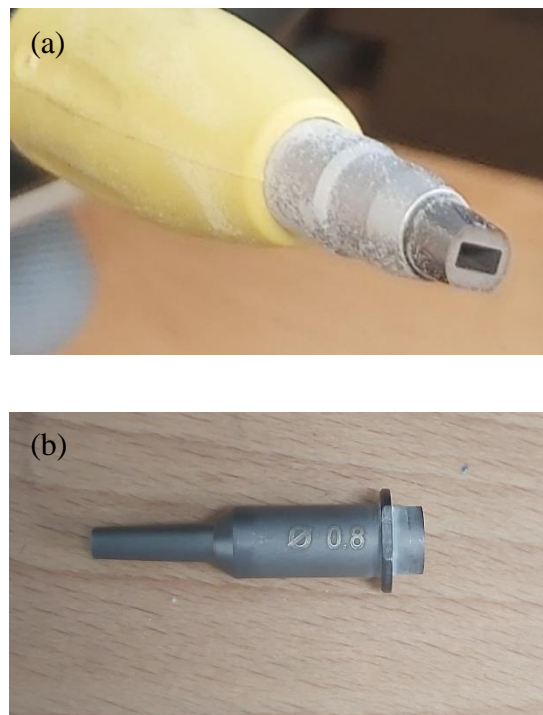
Figure 17. Sand discharge nozzles used; (a) rectangular hole nozzle with dimensions 2.9 x 1.4 mm^2 and in (b) nozzle with the circular hole of diameter 0.8 mm.

A small built in-house stress strain machine was used to evaluate the samples before and after any surface treatment. The second treatment applied to the samples was the electropolishing and that was performed with basic laboratory equipment: a voltage source, a thermometer, a stirring plate, a platinum cathode, an ethanol-nitric acid-based electrolyte and a pair of tweezers used to hold the sample in the electrolyte and to close the electric circuit.
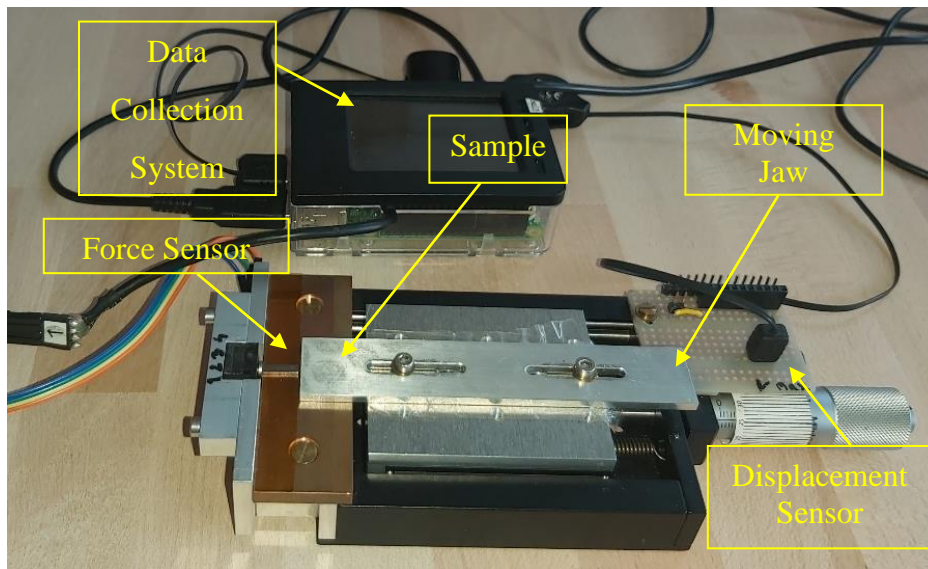
Figure 18. Stress Strain testing device with a sample mounted between the jaws.

Some mechanical polishing was also performed in a couple of the samples in order to reset the surface structure, however that was not part of the standard set of treatments explored in this work. For the mechanical polishing a lapping device was used.

3.6. Results and Discussion:

The first experiments were performed in 4 samples from the same "batch" of material in addition to a longer sample labelled S1 and which was not from the same batch as the others (see **Table 2**). In **Table 2** We can see that sample S1-1 and S1-2, was not subjected to any surface treatments, that is because the samples were already behaving as desired so they were kept so the

behavior of the other samples could be compared with them. The following graph shows the behavior of the untreated samples.
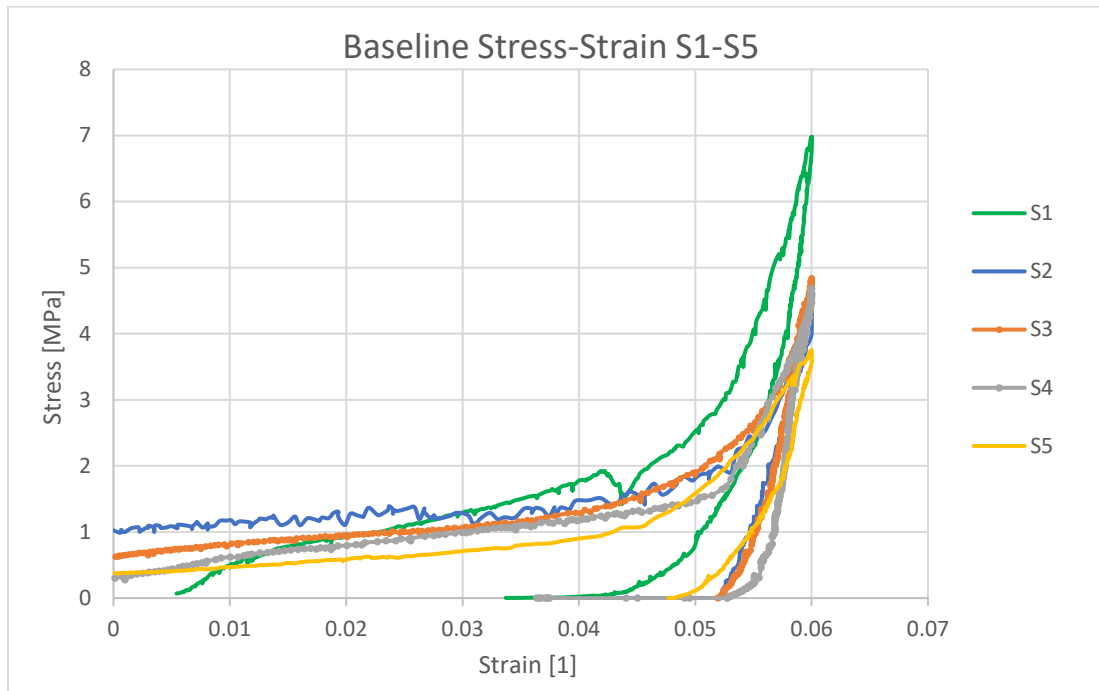
Figure 19. Graph depicting the results of one run for the "Baseline" test for samples S1 through S5.

In **Figure 19**, it is possible to observe that samples S2 and S5 have a lower twinning stress when compared to the other samples, followed by samples S3 and S4, which have slightly higher twinning stress. Finally, sample S1 seems to have the highest twinning stress and a significant spring-back. Sample S1 was being utilized for a pumping application previously so it was previously treated and thus it has some increase in twinning stress caused by the presence of surface damage. However, samples S2 through S5 were not treated in any way and still have significant differences in twinning stresses. This might be an indicator that the samples utilized are not of particularly high quality and probably have a mix of different types of twin boundaries since similar behavior in samples with mixture of different kinds of twin boundaries showed

similar results in previous studies [13]. Bellow a table with all the baseline results and the averages are presented.

Table 3. The table above shows all the results from the baseline test and the averages for twinning stress and spring-back strain.

Sample	Test#	Twinning stress [MPa]	Spring-Back [1]
S1	210623_124701	1.43	0.0174
	210623_123626	1.8	0.0248
	210623_123939	1.79	0.0184
Average		1.67 ± 0.21	0.0202 ± 0.0040
S2	210623_123101	1.48	0.00449
	210623_123626	1.25	0.0073
	210623_123939	1.28	0.0043
Average		1.34 ± 0.10	0.0054 ± 0.0017
S3	210623_143757	1.29	0.006
	210623_144217	1.25	0.007
Average		1.27 ± 0.03	0.0065 ± 0.0007
S4	210623_144903	1.18	0.0055
	210623_145223	1.24	0.008
Average		1.21 ± 0.04	0.01 ± 0.0018
S5	210623_145639	0.9	0.0109
	210623_150054	0.93	0.0132
Average		0.92 ± 0.02	0.0121 ± 0.0016

As shown in **Table 3** the untreated samples have a noticeably smaller spring back as well as a lower twinning stress. However, sample 4 and 5 also seem to have a spring-back higher than the other samples. In the next results I will not be presenting the graphs but only a table with the average results before and after some treatment. But before that, there is still some baselines that have to presented in the following paragraphs.

After this initial test, sample 1 was cut in half to produce two samples, and the sample S6 had a small damaged part on its end cut off. Note that sample S6 was NOT tested yet; **Table 3**, does not present results for sample S6. The halves of sample S1 were labelled as S1-1 and S1-2; those two halves in addition to sample S6 were then tested in the SS machine to produce the results presented in the table below.

Table 4. The table shows the test results for sample 1 after being cut in half and for sample 6 after having a piece on its end cut off. No other treatments were applied to the samples.

Sample #	Twining Stress [MPa]	Spring-Back [1]
S1-1	2.63 ± 0.19	0.009 ± 0.0007
S1-2	2.05 ± 0.075	0.019 ± 0.0052
S6	1.29 ± 0.036	0.003 ± 0

Table 4 clearly shows that there were some differences between the 2 halves of sample S1. They have a significant difference in the amount of spring-back as well as on the magnitude of the twining stress. Looking at the table one could conclude that only sample S1-2 has some potential of working in the pump application. As for sample S6 we have results that would be expected from an untreated sample. The twinning stress is almost half as big as that of sample S1-2, and the amount of spring-back in the sample is very small.

After these "base line" tests, sample S6 was shot peened by hand on both of its T-Faces. This is the test mentioned in the methodology section which was done only for having a "feel" on the necessary pressure for the further shot-peening treatments. This treatment is the one with the parameters illustrated on the first row of **Table 1**.

Table 5. Values for twinning stress and Spring-Back for sample S6 before the shot-peening and after the shot-peening.

S6	Twinning Stress [MPa]	Spring-Back [1]
Before Shot-Peening	1.29 ± 0.036	0.003 ± 0
After Shot-Peening	4.63 ± 0.33	0.023 ± 0.0015

The changes in the materials behavior can be immediately seen in **Table 5**. Before the treatment, the twinning stress of the sample was approximately 1.29 MPa and the amount of spring back was only 0.3%. After the shot-peening, the twinning stress was 4.63 MPa and the spring-back (SB) was 2.3%. While the amount of SB would be satisfactory for a pump application, the twinning stress is too high, since the maximum magneto stress that can be applied to the material is 3 MPa. Such results indicate the excessive damage was caused to the surface of the sample and that this sample was not suitable for the pump application with that amount of damage. This significant change in behavior serves as an indicator that the shot peening treatment should be done in a less harsh manner. That is why further treatments were done with different parameters as described in the methodology section.

Before performing the shot-peening with different parameters, I electropolished samples S2 through S6. **Table 6** bellow shows the results. The electropolishing made sample 6 recover the characteristics it had before the shot-peening, as for the other samples it is possible to observe that mostly they seem to have no change in their characteristics after the electropolishing. For samples 3 through 5 these results might indicate that whatever behavior the sample might have, it is caused

not by some surface modification that can be reverted by electropolishing but rather it is probably caused by other factors present in the sample such as its composition. Note that the results for baseline are the same as the ones presented in **Table 3** (samples S3-5) and **Table 4** (sample S6).

Table 6. Results for average twinning stress and spring-back of samples S2 through S6. In the table there are the baseline results side by side with the results after the electropolishing.

Sample #	Base-Line		After Electropolishing	
	Twinning Stress [MPa]	Spring-Back [1]	Twinning Stress [MPa]	Spring-Back [1]
S2	1.34 ± 0.10	0.0054 ± 0.0017	1.16 ± 0.017	0.004 ± 0.0012
S3	1.27 ± 0.03	0.0065 ± 0.0007	1.16 ± 0.118	0.005 ± 0.0010
S4	1.21 ± 0.04	0.01 ± 0.0018	1.31 ± 0.006	0.004 ± 0.0010
S5	0.92 ± 0.02	0.0121 ± 0.0016	1.12 ± 0.053	0.008 ± 0.0010
S6	1.29 ± 0.036	0.003 ± 0	1.31 ± 0.068	0.002 ± 0.0006

As observed table in **Table 7**, the treatments with the parameters shown in row 2 of **Table 1**, resulted in promising results. It is possible to observe that the base-line twinning stresses were around 1 MPa for all three samples. After the shot-peening only one side of each of the samples, the twinning stress for all of them is at least 2 MPa. Such results are in agreement with previously reported results in source [5].

Table 7. The table shows the baseline results side by side with the results after shot-peening, with the parameters shown in row 2 of **Table 1**.

Sample #	Base-Line		After Shot-Peening	
	Twinning Stress [MPa]	Spring-Back [1]	Twinning Stress [MPa]	Spring-Back [1]
S3	1.27 ± 0.03	0.0065 ± 0.0007	2.07 ± 0.08	0.023 ± 0.005
S4	1.21 ± 0.04	0.01 ± 0.0018	2.19 ± 0.17	0.025 ± 0.005
S5	0.92 ± 0.02	0.0121 ± 0.0016	2.14 ± 0.12	0.026 ± 0.001

Based on the results in the table from **Table 7**, all the samples seem to be promising as far as the utilization in the microfluidic pump is concerned. However, I moved on with electropolishing the sample to perform more tests with different parameters of the shot-peening.

Table 8. The table shows the baseline results compared to the results after electropolishing.

Sample #	Base-Line		After Electropolishing	
	Twinning Stress [MPa]	Spring-Back [1]	Twinning Stress [MPa]	Spring-Back [1]
S3	1.27 ± 0.03	0.0065 ± 0.0007	1.35 ± 0.01	0.015 ± 0.00
S4	1.21 ± 0.04	0.01 ± 0.0018	1.33 ± 0.06	0.011 ± 0.00
S5	0.92 ± 0.02	0.0121 ± 0.0016	1.28 ± 0.25	0.015 ± 0.00

From the results shown in **Table 8** we can see that the electropolishing once again was able to recover the previous properties of the samples. However, by comparing the results with the base-line we can see that the twinning stress and spring-back are still somewhat higher. This is probably just because the electropolishing was not done for long enough to completely remove the surface affected by the shot-peening treatment. However, the results are close enough to the base-line that the samples were deemed good enough to be retreated.

Table 9. This table shows the values for Twinning-Stress and Spring-Back for the Baseline test and After the Shot-peening. The shot-peening in this case was performed with the parameters show in row 3 of **Table 1**.

Sample #	Base-Line		After Shot-Peening	
	Twinning Stress [MPa]	Spring-Back [1]	Twinning Stress [MPa]	Spring-Back [1]
S4	1.21 ± 0.04	0.01 ± 0.0018	1.63 ± 0.01	0.009 ± 0.0016

The results show in **Table 9** are somewhat odd when compared to the results obtained after electropolishing in **Table 8**. While the twinning stress has increased, as was expected to happen, the amount of spring-back stayed relatively constant, and was in fact lower than what was measured after the electropolishing. Such results were very unusual and I suspect some measuring equipment issue. Given this unexpected behavior I decided to utilize sample 4 for the pump application despite the results obtained with the last treatment (**Table 9**). I decided to do that because the twinning stress was still lower than what I had measured previously with the shot-peening at 1.5 Bar pressure.

3.7. Conclusion:

There are a few noteworthy points from the previous discussion. First it is evident that the parameters used for the shot-peening treatment has an effect not only on the shape of the stress strain curve of any given sample, but also it has a significant effect on the magnitude of the twinning stress. Another thing that becomes evident from shot-peening the samples with different pressure parameters, is that the damage caused to the surface of the sample is strongly dependent on the air pressure and on the size of the discharge nozzle. Although this was not tested in this work, I would expect that the surface damage is also dependent on the speed with which the sample

moves under the sand stream. If that is the case, that could give some flexibility for others trying to perform the same kind of treatments, but that can easily control only 1 or 2 of the variables but not all of them, thus being able to achieve the same results controlling different parameters. This is only a hypothesis and I have not collected any data for exploring that matter in the present work.

The results obtained with different shot-peening parameters is summarized in the table below. No results for the electropolishing are presented because the electropolishing did not significantly change the values of spring-back and twinning stress when compared to the base-line results.

Table 10. Summary of the results obtained with different treatment parameters for samples S3 through S5 compared to the base-line results.

Sample #	Base-Line		Shot-Peening 1.5 bar		Shot-Peening 1 bar	
	Twinning Stress [MPa]	Spring-Back [1]	Twinning Stress [MPa]	Spring-Back [1]	Twinning Stress [MPa]	Spring-Back [1]
S3	1.27 ± 0.03	0.0065 ± 0.0007	2.07 ± 0.08	0.023 ± 0.005	NA	NA
S4	1.21 ± 0.04	0.01 ± 0.0018	2.19 ± 0.17	0.025 ± 0.005	1.63 ± 0.01	0.009 ± 0.0016
S5	0.92 ± 0.02	0.0121 ± 0.0016	2.14 ± 0.12	0.026 ± 0.001	NA	NA

From the results in the previous section, we can also see that the electropolishing seems to not induce any surface defects that can be used to change the properties of the material, at least not when we are concerned with twinning stress and the general shape of the stress strain curve. This is in conformity with some previous works that have used electropolishing as a way of removing any residual surface stresses [13]. By removing major surface defects from the samples, one can treat the same sample with different procedures repeatedly.

Finally, although the spring-back amount of the sample S4 seems to be very low from the results in **Table 9**, I was not able to find in the literature a recommendation for the amount of spring-back to obtain a consistent pump. My hypothesis is that although the presence of spring-back is a prerequisite for a suitable sample, how much of a spring-back is present affects the pumping characteristics and the overall performance of the microfluidic pump, however such hypothesis was not investigated here. Thus, I decided to use sample S4 for the construction of the microfluidic pump which will be described in the following section. The decision of using sample S4 was taken because the twining stress was lower than what we obtained in the same sample with different treatment parameters. In addition to that, I suspected measurement errors on the amount of spring-back recorded, and I was not able to find information in the literature about what amount of spring-back that is necessary to obtain a reliable pump; finally, the results displayed in **Table 7** have very promising characteristics for working in a pump application, therefore I was confident that I had already stablished a method for obtaining samples that would be successful for the microfluidic pump application. In the next section I will go in detail on how the sample was utilized as the active part of a microfluidic pump, and then I will talk about the design and construction of a working prototype of a microfluidic pump.

4. Designing a Microfluidic Pump:

In this section the design of the pump will be presented, as well as the requirements to install the MSMA sample properly so the pump functions as desired. I will also briefly comment on the process for production of parts made out of PDMS. There will also be presented some newer improvements on the pump design which will be explored in the future.

4.1. Installation of MSM Element:

The MSM part has to be properly constrained in order to perform as desired in the pump. Proper constraint and prevention of leaks is essential for an optimized and reliable functioning of the device [12]. The challenge was to propose a pump design that could be assembled in such a way that those two criteria would be reliably met while allowing for the interchangeability of MSM elements being utilized in the pump. As mentioned in section **2.3**, this property would allow the pump to be used for other purposes, such as a testing device for how other material parameters can affect the performance of a MSM sample, in addition to serving as a fluidic device for demonstrations of MSMA's applications.

For the proper constraining of the MSMA element it is necessary to use a stiff material to seat against the T-Faces (see **Figure 11**) of the sample. For the sealing the silicone elastomer Dow Corning, Sylgard 184 was used. The material must not only provide good sealing capabilities but it must also not be so stiff as to prevent the MSMA sample from expanding during actuation. As reported in [12], the PDMS, when prepared with the recommended mixing ratios, is still too stiff to allow for proper actuation of the pump. Thus, the PDMS on the ends of the samples was cutoff and a softer silicone material was applied to replace it. For the pump produced in the present work the silicone used was the Ceresit CS25 sanitary silicone.

4.2. Pump Construction:

There were a couple of iterations to get to a functional pump design. Initially my design was made in such a way that the MSM sample was surrounded by PDMS as a sealant material, but eventually that was changed because the PDMS was too stiff. The general initial design I utilized for the pump was enough to obtain a functional prototype, however there are certainly many improvements that could be made.

ITEM	QTY	PART NUMBER	DESCRIPTION
1	1	MotorBox Lid	
2	1	micro-metal-gearmotor-standard	STEP AP214
3	1	PumpFrame	
4	1	Magnet Shaft holder	
5	1	Magnet	
6	1	MSMA holder	
7	1	PDMS for MSM sample	
8	1	Channel Plate	
9	1	Channel Holder	
10	1	Pressure Cap	

Designed by: Gabriel B. Parreira — Date: 20/04/2022 — PumpExploded — Sheet 1 / 1
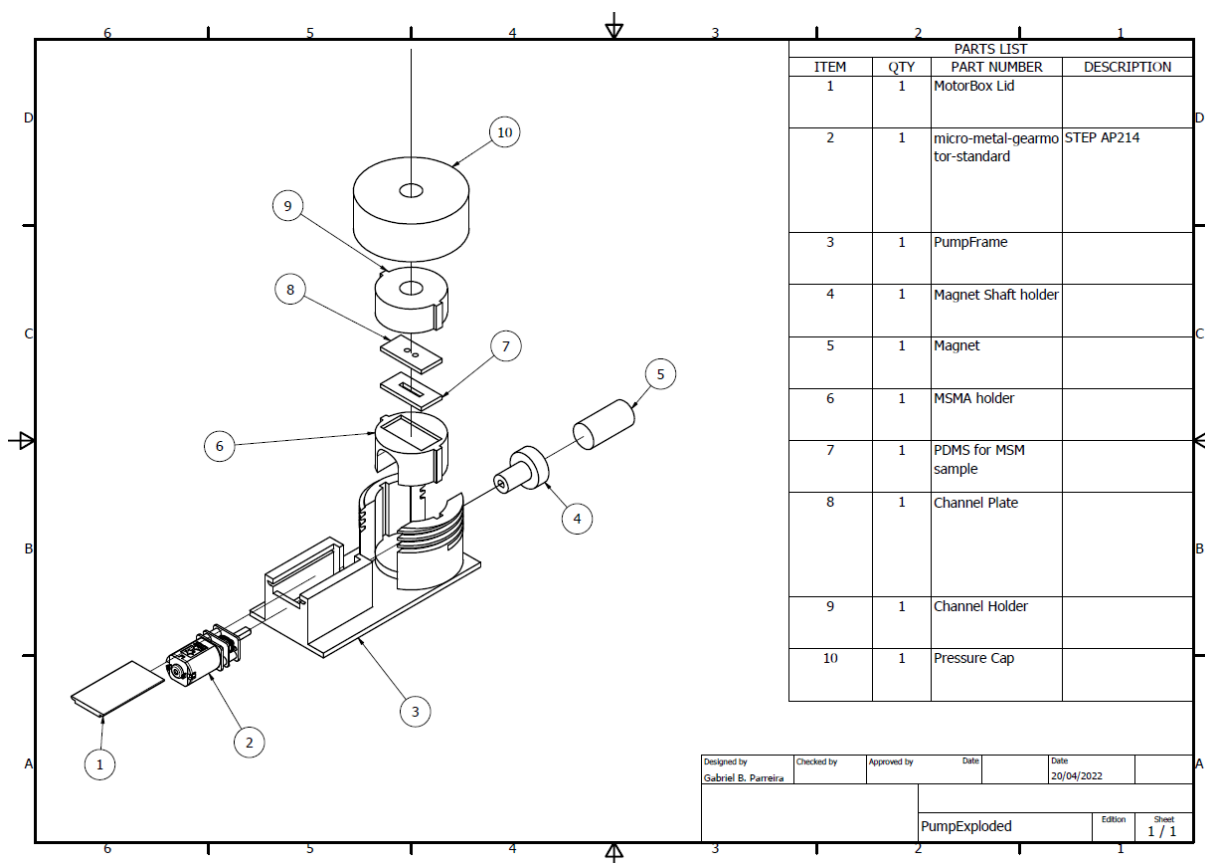
Figure 20. Assembly drawing of the original pump design. The MSM element is not included in this assembly.

The pump consists of a frame with a box for the motor as well as a cavity with external trapezoidal threads where the other parts containing the MSM sample will be contained. For attaching the diametrically magnetized magnet I made a small shaft with a cavity where the magnet

is press fitted, and on the other end there is a cavity where the shaft of the motor can be press-fitted as well. There is a support for the MSM element in which the PDMS sealant material is placed, and on top of that there is a plate with small orifices through which a fluid can flow when the pump is working. Then there is another cap that covers the "channel plate" and finally there is a threaded cap that can be used to apply pressure to the channel plate and allow for sealing of the PDMS against the channel plate. The separation into two parts of the pressing mechanism was so that the part immediately above the channel plate would not spin as the threaded cap is being screwed in. That allows for an easier alignment of the channels with the MSMA element. The threads were chosen as trapezoidal to guarantee the strength of the parts as they were all 3D printed and therefore are hollow to some degree. Also, since the surface of a 3D printed part is very rough, it was assumed that despite the trapezoidal thread, there was still enough friction to securely maintain the cap in place, and indeed there were no issues with the cap unscrewing itself.

4.2.1. PDMS Preparation:

The PDMS material used for sealing in the pump is sold as a 2-part liquid silicone material. When the 2 parts are mixed the silicone hardens to form a solid material. This solidification can be sped up by UV light or by heating up the silicone mix. The recommended mixing ratio is 10 parts of the "base" PDMS polymer to 1 part catalyst, but the mechanical properties of the final solid PDMS can be modified according to curing temperatures and time as well as the mixing ratio used [14]. For the pump in this work, I used the conventional 10:1 mixing.
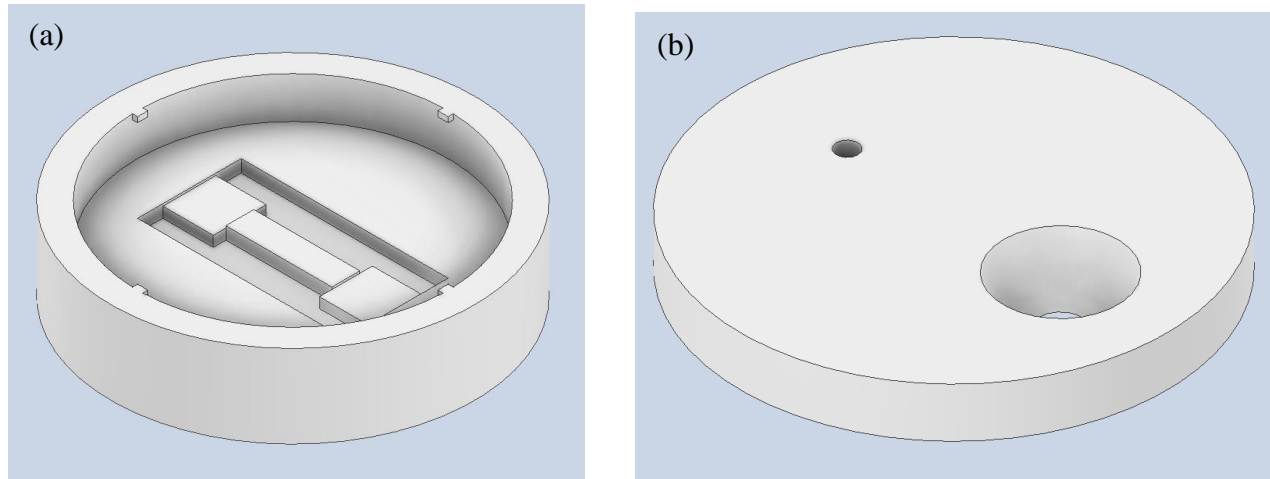
Figure 21. Mold used for making the PDMS parts. In (a) there is the bottom of the mold with the core in shape of the MSM element and the ends making a cavity for addition of the sanitary silicone, and (b) top part of the mold with pouring port and a vent hole.

To achieve the desired thickness of the sealant material, a mold was designed with a core that replicated the geometry of the MSMA part. A FDM printer was used to make the mold. The material used to make the mold was PETG plastic. The mold is depicted in **Figure 21** above. Other molds were designed with different printing techniques, but the one shown in **Figure 21** was the one used to make the PDMS seal for the working pump prototype. The PDMS was mixed and poured into this mold, then it was left to cure in an oven at 60 °C for approximately 2 hours. Once the PDMS was cured the mold could then be removed and the MSMA part was then installed with the sealant material in the pump. Then the softer silicone was applied on the edges of the MSMA part and the application of the sealant material was thus complete, and the MSM was ready to be used in the pump.

4.3. Results and discussion:

Upon testing the pump with sample S4, I was able to observe that the fluid transfer was occurring from one channel to the other. The sequence of photos bellow illustrates that.
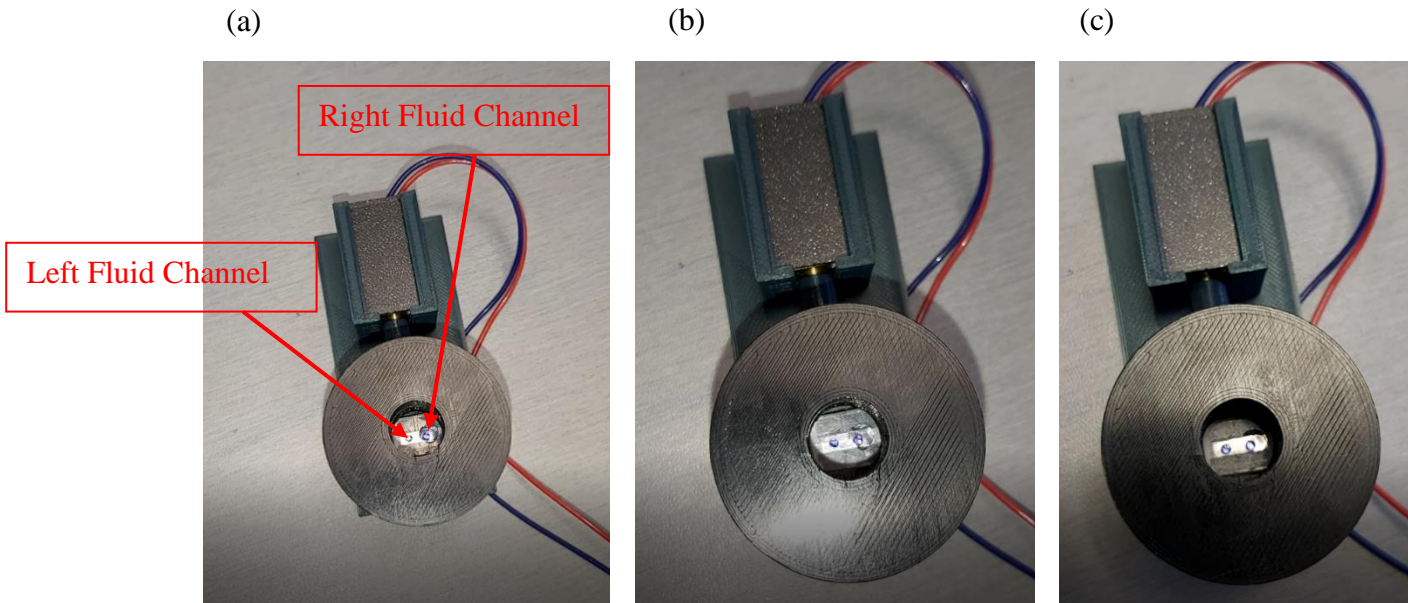
Figure 22. Sequence of frames from a recording of the working pump to illustrate the transference of fluid. (a) most of the fluid in the right channel; (b) some fluid transferred from right to left, and (c) most of the fluid in the left channel. For more details on the parts of the pump refer back to **Figure 20** as this pump construction is mostly the same as the one depicted there.

Although the pump worked as desired, unfortunately I was unable to prepare a proper set up to test quantitative characteristics of the pump. As a consequence of that, the only data I was able to obtain on the working of the pump was the visual observation of successful fluid transfer. A new design to address that and other issues was made but it has yet to be tested. This design solves the issue of testing by including in the design a place where fluidic fittings can be directly attached to the pump and used for connecting to a testing device. The pump frame, as indicated in **Figure 20**, was not changed.

PARTS LIST		
ITEM	QTY	PART NUMBER
1	1	MSMA Holder Bottom
2	1	MSMA Holder Top
3	1	Channel Plate
4	1	Pressure Cap
5	1	Sample
6	1	Connection Interface
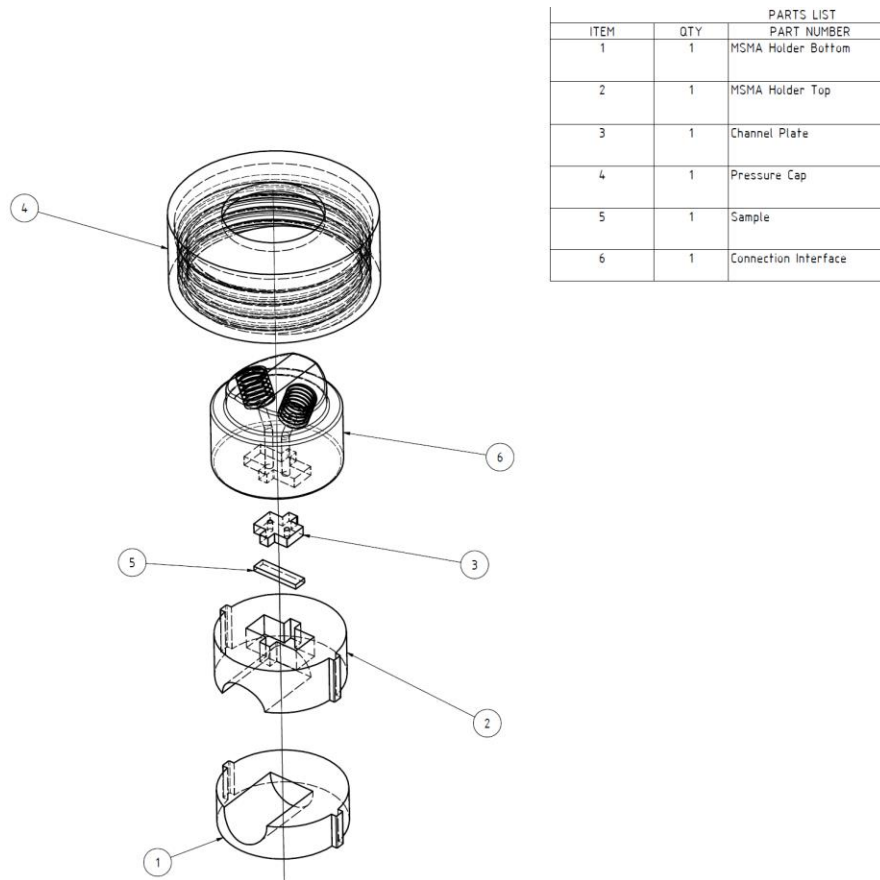
Figure 23. Exploded view of the modified design for the active region of the pump.

The main changes in the design presented in **Figure 23** when compared to the older version, is that in this new design the magnet is also supported on the bottom to allow it to stay better aligned when it rotates. The geometry of the channel plate, the MSM cavity and the part that previously held the channel plate all changed. In this design the top part that previously held the channel plate also has the fluidic channels inside of it, and it possesses an integrated connection interface; this allows for direct connection of M6 fittings to the pump. The top cap also changed slightly, but only to allow the top of the part with the fittings to go over it so the tubes can be connected to the pump. It is also my intention to change the procedure of casting the PDMS that will be used as sealant in this new design.

A solution to the PDMS stiffness, is to use a different mixing ratio for the PDMS production. Previous studies showed that changing the mixing ratio of the PDMS parts can decrease the stiffness of the material to values as low as 800 kPa [14], and it might be possible to go even lower by adjusting the mixing ratios. Although 800 kPa is lower than the stiffness obtained with the recommended mixing ratios, it is still higher than the stiffness of the sanitary silicone used in the pump, which should have stiffness of approximately 300 kPa [15]. I will explore the viability of using the softer PDMS in later investigations.

4.4. Conclusion:

The MSMA-based micropump produced in this work was made with the objective of demonstrating the applications of MSMA materials and to be used as cycle tester. The cycle testing application would be made possible by the fact that the active part utilized in the pump could be replaced by a different active MSM element. Although there was not an opportunity to make a quantitative evaluation (i.e., flow rate and achievable pressure) of the pump constructed, it was possible to observe that the pump was successfully transporting fluids and actuating the MSMA sample installed in it. Thus, the original purpose of the pump was appropriately fulfilled, as what was needed from it was only a visually observable functionality and proper actuation of samples to cycle test.

Despite having the basic requirements of the pump fulfilled, more work will be done to improve the design and to allow for a quantitative test of flow rate and pumping pressure. It would also be desirable to use only the PDMS as a sealant instead of having to rely on the sanitary silicone, and that will also be further explored in the future. Finally, a more robust construction for containing the electronic controls of the pump would also be a desirable, albeit secondary, thing to be done, as well as making the part housing the MSMA sample out of some transparent material.

5. General Evaluation and Conclusion:

The present bachelor's thesis proposed to explore the effects of surface treatments on the twinning stress and spring-back of the NiMnGa magnetic shape memory alloy, and to construct a functional microfluidic pump based on the magnetic actuation of this alloy for demonstration purposes and for possible cycle testing application. In **section 2** the effects of the shot-peening treatment were presented in addition to how changes to the parameters of such treatment affected the twinning stress and spring-back of the material studied. It was also studied and presented how the electropolishing affected those two parameters.

From those results it was possible to observe that the shot-peening treatment had different results based on the size of the orifice used for discharging the sand as well as on the air pressure in the device. And for electropolishing it was concluded that the process did not significantly affect the twinning stress of the material, unless there was already some significant damage present on the surface and which was then removed by the electropolishing. In these terms, the evaluation of the effects of surface treatment on twinning stress was successfully evaluated in the present work. The table below is showing the specific results obtained with the different pressures utilized for the shot-peening. This table is a copy of **Table 10**. Once again electropolishing results are not depicted as they did not produce a change when compared to the base-line results.

Table 10. Summary of the results obtained with different treatment parameters for samples S3 through S5 compared to the base-line results.

Sample #	Base-Line		Shot-Peening 1.5 bar		Shot-Peening 1 bar	
	Twinning Stress [MPa]	Spring-Back [1]	Twinning Stress [MPa]	Spring-Back [1]	Twinning Stress [MPa]	Spring-Back [1]
S3	1.27 ± 0.03	0.0065 ± 0.0007	2.07 ± 0.08	0.023 ± 0.005	NA	NA
S4	1.21 ± 0.04	0.01 ± 0.0018	2.19 ± 0.17	0.025 ± 0.005	1.63 ± 0.01	0.009 ± 0.0016
S5	0.92 ± 0.02	0.0121 ± 0.0016	2.14 ± 0.12	0.026 ± 0.001	NA	NA

Although electropolishing did not affect the twinning stress when compared to base-line, below there is an additional table that shows how the electropolishing effectively reverted the effects of shot-peening.

Table 11. Results after shot-peening of samples S3 through S5 at 1.5 bar air pressure, and the results obtained by electropolishing after that shot-peening treatment.

Sample #	After Shot-Peening		After Electropolishing	
	Twinning Stress [MPa]	Spring-Back [1]	Twinning Stress [MPa]	Spring-Back [1]
S3	2.07 ± 0.08	0.023 ± 0.005	1.35 ± 0.01	0.015 ± 0.00
S4	2.19 ± 0.17	0.025 ± 0.005	1.33 ± 0.06	0.011 ± 0.00
S5	2.14 ± 0.12	0.026 ± 0.001	1.28 ± 0.25	0.015 ± 0.00

Concerning the construction of the pump, it was possible to make a functional pump that transferred fluid and that actuated the sample. However, the need of utilizing the sanitary silicone jeopardizes the reusability of the pump for other samples. Having this in mind, it can be said that making a demonstration prototype of the pump was accomplished, but the possibility of using that

device as some sort of cycle tester was not successful. Many design improvements were already proposed, and some changes to the PDMS were equally suggested to make this last point possible, but unfortunately those improvements will only be explored later and could not make it to the present thesis.

Reference:

[1]   SMITH, AARON R.: New methods for controlling twin configurations and characterizing twin boundaries in 5M Ni-Mn-Ga for the development of applications : Lappeenranta University of Technology, 2015. — Accepted: 2015-06-09T05:13:08Z — ISBN 978-952-265-808-1

[2]   ARMSTRONG, ANDREW: Material Design, Processing, and Engineering Requirements for Magnetic Shape Memory Devices. In: Boise State University Theses and Dissertations (2020)

[3]   ULLAKKO, K. ; WENDELL, L. ; SMITH, A. ; MÜLLNER, P. ; HAMPIKIAN, G.: A magnetic shape memory micropump: contact-free, and compatible with PCR and human DNA profiling. In: Smart Materials and Structures Bd. 21, IOP Publishing (2012), Nr. 11, S. 115020

[4]   ZHANG, HU ; ARMSTRONG, ANDREW ; MÜLLNER, PETER: Effects of surface modifications on the fatigue life of unconstrained Ni-Mn-Ga single crystals in a rotating magnetic field. In: Acta Materialia Bd. 155 (2018), S. 175–186

[5]   CHMIELUS, MARKUS ; WITHERSPOON, CASSIE ; ULLAKKO, KARI ; MÜLLNER, PETER ; SCHNEIDER, RAINER: Effects of surface damage on twinning stress and the stability of twin microstructures of magnetic shape memory alloys. In: Acta Materialia Bd. 59 (2011), Nr. 8, S. 2948–2956

[6]   BRAGHERI, FRANCESCA ; MARTÍNEZ VÁZQUEZ, REBECA ; OSELLAME, ROBERTO: Chapter 12.3 - Microfluidics. In: BALDACCHINI, T. (Hrsg.): Three-Dimensional Microfabrication Using Two-Photon Polymerization (Second Edition), Micro and Nano Technologies : William Andrew Publishing, 2020 — ISBN 978-0-12-817827-0, S. 493–526

[7]   LEE, CHANG-SOO: Grand Challenges in Microfluidics: A Call for Biological and Engineering Action. In: Frontiers in Sensors Bd. 1 (2020)

[8]   NIELSEN, ANNA V. ; BEAUCHAMP, MICHAEL J. ; NORDIN, GREGORY P. ; WOOLLEY, ADAM T.: 3D Printed Microfluidics. In: Annual Review of Analytical Chemistry Bd. 13 (2020), Nr. 1, S. 45–65

[9]   CHIU, DANIEL T. ; DEMELLO, ANDREW J. ; DI CARLO, DINO ; DOYLE, PATRICK S. ; HANSEN, CARL ; MACEICZYK, RICHARD M. ; WOOTTON, ROBERT C. R.: Small but Perfectly Formed? Successes, Challenges, and Opportunities for Microfluidics in the Chemical and Biological Sciences. In: Chem Bd. 2 (2017), Nr. 2, S. 201–223

[10]   Comparison between peristaltic, syringe and pressure pumps for microfluidic applications - Fluigent. URL https://www.fluigent.com/resources-support/expertise/expertise-reviews/what-is-microfluidics/comparison-between-peristaltic-syringe-and-pressure-pumps-for-microfluidic-applications/. - abgerufen am 2022-06-09. — https://www.fluigent.com/

[11]   ZHAO, BEI ; CUI, XINGYE ; REN, WEI ; XU, FENG ; LIU, MING ; YE, ZUO-GUANG: A Controllable and Integrated Pump-enabled Microfluidic Chip and Its Application in Droplets Generating. In: Scientific Reports Bd. 7, Nature Publishing Group (2017), Nr. 1, S. 11319

[12]   SAREN, A. ; SMITH, A. R. ; ULLAKKO, K.: Integratable magnetic shape memory micropump for high-pressure, precision microfluidic applications. In: Microfluidics and Nanofluidics Bd. 22 (2018), Nr. 4, S. 38

[13]   MUSIIENKO, DENYS ; NILSÉN, FRANS ; ARMSTRONG, ANDREW ; RAMEŠ, MICHAL ; VEŘTÁT, PETR ; COLMAN, ROSS H. ; ČAPEK, JAROSLAV ; MÜLLNER, PETER ; U. A.: Effect of crystal quality on twinning stress in Ni–Mn–Ga magnetic shape memory alloys. In: Journal of Materials Research and Technology Bd. 14 (2021), S. 1934–1944

[14]   SEGHIR, R. ; ARSCOTT, S.: Extended PDMS stiffness range for flexible systems. In: Sensors and Actuators A: Physical Bd. 230 (2015), S. 33–39

[15]   ceresit-global-cs25-sanitary-silicone-tds.pdf.

Figures List:

Tables List: